Optimal Resource Allocations for Statistical QoS Provisioning in Supporting mURLLC Over FBC-EH Based 6G THz Wireless Nano-Networks

Xi Zhang, *Fellow, IEEE*, Jingqing Wang, and H. Vincent Poor, *Life Fellow, IEEE*

***Abstract*—While 5G is being deployed around the world, the efforts and initiatives from academia, industry, and standard bodies have started to conceptualize 6G mobile wireless networks and propose various promising 6G techniques in supporting very stringent quality-of-service (QoS) requirements. Inspired by the new and important service class of the massive Ultra-Reliable Low-Latency Communications (mURLLC), finite blocklength coding (FBC) has been shown to significantly improve various QoS performances by using short-packet communications. On the other hand, Terahertz (THz) band nano communications have been widely envisioned as a promising 6G technique to efficiently support ultra-high data-rate (up to 1 Tbps). One of the major constraints over THz-band nano-networks is the severely limited energy that can be accessed by nano devices. Towards this end, various novel energy harvesting (EH) mechanisms have been proposed to remedy the energy scarcity problem. However, how to accurately characterize the relationships among THz wireless channel, energy consumption, and EH models for FBC based nano communications still remains as a challenging problem to support statistical delay and error-rate bounded QoS provisioning over FBC based 6G THz wireless nano-networks. To overcome these challenges, we propose optimal resource allocation policies to achieve the maximum ϵ-effective capacity in the THz band over FBC-EH-based nano-networks. Particularly, we establish nano-scale system models and characterize wireless channel models in the THz band using FBC. Considering statistical delay and error-rate bounded QoS provisioning, we formulate and solve the ϵ-effective capacity maximization problem under several different EH constraints for our proposed schemes. Simulation results are included, which validate and evaluate our proposed schemes in the finite blocklength regime.**

***Index Terms*—Statistical delay and error-rate bounded QoS, THz band, mutual information, FBC, energy harvesting, joint resource allocation, ϵ-effective capacity, 6G wireless nano-networks.**

I. Introduction

WHILE 5G is being deployed around the world, the efforts and initiatives from academia, industry, and standard bodies have started to look beyond 5G, conceptualize 6G mobile wireless networks, and propose various promising 6G techniques in supporting very stringent quality-of-service (QoS) requirements [1–8] for wireless networks, including ultra-high data-rate ($\approx$1 Tbps), bounded end-to-end delay (< 1 ms), super-reliability ($> 99.99999\%$), extra-high energy efficiency, etc. [9] [10] [11]. Correspondingly, 6G defines a new and important service class of the *massive Ultra-Reliable Low-Latency Communications* (mURLLC) to quantitatively design and evaluate its QoS performances. In this context, Terahertz (0.1–10 THz) band communications and wireless networks have been widely envisioned as the promising 6G wireless techniques to efficiently support stringent QoS requirements of mURLLC. This is because THz wireless networks with nano-architectures can alleviate the spectrum scarcity and feasibly achieve ultra-high data-rates up to 1 Tbps, while taking into account constraints of scalability, dimension, topology, processing-power, storage, energy capacities, etc.

Inspired by the new service class mURLLC, finite blocklength coding (FBC) has been proposed [12–15] to support both latency and reliability requirements for time-sensitive wireless services by using short-packet data communications. The authors of [12] have shown that the codeword blocklength can be as short as 100 channel symbols for reliable communications, which significantly reduce the latency while efficiently upper-bounding the error rate. The authors of [16] have studied different properties of channel codes that approach the fundamental limits of a given memoryless wireless channel in the finite blocklength regime. The maximum achievable coding rate using FBC over Additive white Gaussian noise (AWGN) channels has been derived in [17].

On the other hand, the limited available bandwidth for communication systems in the microwave frequency range motivates the exploration of higher frequency bands in supporting statistical delay-bounded QoS provisioning. Towards this end, researchers have proposed the millimeter wave (mmWave) communication systems. Despite the much higher operation frequency, the available band on frequency is less than 10 GHz, which requires the communication systems to achieve a *spectral efficiency* on the order of 100 bits/second/Hz for supporting 1 Terabit-per-second (Tbps) for 6G wireless networks [18] [19]. However, this is several times above the state-of-the-art for wireless communication systems. To satisfy the increasing demand for higher-speed of current wireless systems, THz band communication techniques [20] [21] have been proposed to provide an unprecedentedly large bandwidth, ranging from several tens of GHz up to a few THz, while

Manuscript received Jul. 12, 2020; revised Nov. 22, 2020; accepted Mar. 1, 2021. The work of Xi Zhang and Jingqing Wang was supported in part by the U.S. National Science Foundation under Grants CCF-2008975, ECCS-1408601, and CNS-1205726, and the U.S. Air Force under Grant FA9453-15-C-0423. The work of H. Vincent Poor was supported in part by the U.S. National Science Foundation under Grant CCF-0939370 and Grant CCF-1908308. (Corresponding Author: Xi Zhang.)

Xi Zhang and Jingqing Wang are with the Networking and Information Systems Laboratory, Department of Electrical and Computer Engineering, Texas A&M University, College Station, TX 77843 USA (e-mail: xizhang@ece.tamu.edu; wang12078@tamu.edu).

H. Vincent Poor is with Department of Electrical Engineering, Princeton University, Princeton, NJ 08544 USA (e-mail: poor@princeton.edu).

satisfying the increasing demand of 100 Gbps and even 1 Tbps data rates [22]. However, the large pathloss and molecular noise introduced by the THz wireless systems may produce transmission errors during the data transmissions, resulting in distorted multimedia signals received. Therefore, it is crucial to apply the FBC technique for short-packet data transmissions to support time-sensitive wireless services while guaranteeing statistical both delay and error-rate bounded QoS provisioning in the THz band. Previous works have presented a holistic vision of 6G systems for the 6G-driven applications, performance metrics, and new service classes such as THz, mURLLC, QoS metrics, etc. [9]. However, previous works mainly focus on analyzing specific QoS requirements, while the statistical QoS provisioning based THz-band communications in supporting mURLLC have neither been well understood nor thoroughly studied.

Motivated by the potential of THz technologies, researchers have focused on leveraging the advantages of nanomaterials, such as graphene [23–26], to implement THz communication systems into a set of applications. There has been a limited number of studies on the channel characterisation of THz-band nano-communication systems, which incorporate molecular absorption, spreading loss, and shadowing into a theoretical THz channel model [27] [28]. The authors of [29] have reviewed the current state-of-the-art technologies and applicability of nano communication in biomedical application. The authors of [30] have shown that the large bandwidth in the THz band is susceptible to shadowing and noise. The joint effects of path loss and shadowing for THz wireless channels have been studied in [31]. The channel modelling of the THz wave propagating and the corresponding channel capacity modelling with different power allocation schemes for electromagnetic communications have been studied in [32]. The channel capacity in the THz band is numerically evaluated by using a new THz-band propagation model with different channel molecular compositions and under different power allocation schemes in [33].

Furthermore, one of the major constraints of wireless nano-networks is the severely limited energy that can be accessed by nano devices. As a result, researchers have investigated the energy harvesting (EH) techniques over THz band wireless nano-networks. However, the conventional EH techniques, such as solar and wind power, cannot be utilized in wireless nano-networks due to technology limitations. Novel nano-scale EH techniques have been investigated to harvest energy from various resources, such as vibration and blood sugar, to address the energy scarcity problem for nano devices. The authors of [34] have conducted detailed studies of EH techniques, energy sources, storage technologies, and the examples of applications and network deployments for EH based nano sensors. Optimal energy management policies for EH based sensor nodes have been proposed in [35]. Although there are some studies of the EH and energy consumption models for nano-scale communications, how to accurately model and characterize the relationships among THz-band wireless channel, energy consumption, and EH models employing FBC based nano-communication still remains as a major challenge in the THz band while supporting both delay and error-rate bounded QoS provisioning.

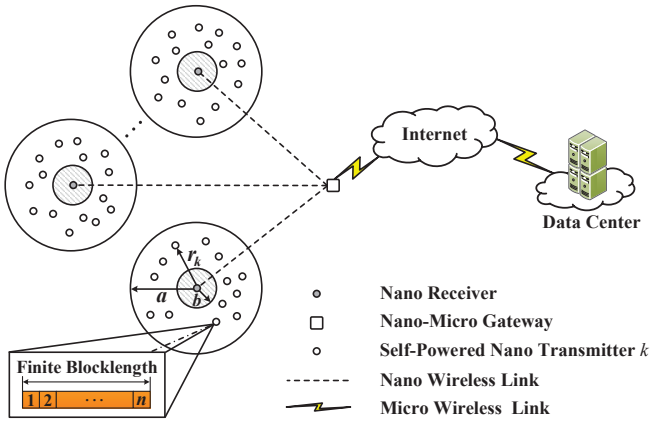

Fig. 1. The system architecture model for our proposed FBC-EH-based wireless nano-networks in the THz band, where a is the radius of the THz-band covered region, b is the radius of the blind area, and n is the codeword blocklength used in FBC.

To effectively overcome the above-mentioned challenges, in this paper we develop FBC-EH based optimal resource allocation policies for *self-powered* nano devices in the THz band over wireless nano-networks under statistical delay and error-rate bounded QoS constraints. Particularly, we establish THz-band wireless communications model, EH model, and FBC based channel-coding model. Then, we analyze the interference, channel capacity, and channel dispersion functions in the THz band using FBC. Considering statistical delay and error-rate bounded QoS provisioning, we formulate and solve the ϵ-effective capacity maximization problem for our proposed statistical delay and error-rate bounded QoS provisioning in supporting mURLLC over FBC-EH based 6G THz wireless nano-networks. Simulations are conducted, which evaluate and validate our proposed schemes in the THz band over FBC-EH-based wireless nano-networks.

The rest of this paper is organized as follows: Section II establishes THz-band nano communication system models. Section III characterizes the interference, channel capacity, and channel dispersion in the THz band using FBC. Section IV formulates and solves the ϵ-effective capacity maximization problem under statistical delay and error-rate bounded QoS provisioning in the finite blocklength regime in the THz band. Section V evaluates the system performance for our proposed schemes in the THz band in the finite blocklength regime. The paper concludes with Section VI.

II. The System Models

Fig. 1 shows the system architecture model for our proposed FBC-EH-based wireless nano-networks in the THz band, where for each THz-band covered region in a circled area, a is the radius of the THz-band covered region and b is the radius of a very small blind area ($b \ll a$), and there is one nano receiver and $(K+1)$ self-powered nano transmitters, without the use of nano-batteries, randomly distributed within the THz-band covered region, which follows a spatial Poisson process with an arrival-rate intensity equal to λ nodes/cm^2 [36]. Consider the THz-band covered region, denoted by $A(a) \subseteq \mathbb{R}^2$,

with radius a. Without loss of generality, we consider that the nano receiver is located at the center of the THz-band covered region $A(a)$. We can derive the probability of finding $(K+1)$ nano transmitters in the THz-band covered region $A(a)$ as follows:

$$\begin{aligned}&\Pr\{(K+1) \text{ nano transmitters in } A(a)\}\\&= \frac{[\lambda \|A(a)\|_\phi]^{(K+1)}}{(K+1)!} \exp\left[-\lambda \|A(a)\|_\phi\right] \end{aligned} \tag{1}$$

where $\|A(a)\|_\phi$ denotes the area of the THz-band covered region $A(a)$. Denote by r_k $(k = 1, \ldots, (K+1))$ the transmission distance from the self-powered nano transmitter k, as shown in Fig. 1, to its assigned nano receiver within the THz-band covered region, which is a random variable. Then, we can formulate the probability density function (PDF) of the distribution of transmission distance r_k, denoted by $f_D(r_k)$, from the nano transmitter k to its nano receiver of interest within the THz-band covered region as follows [37]:

$$f_D(r_k) = \begin{cases} \frac{2r_k}{a^2-b^2}, & \text{for } b < r_k < a; \\ 0, & \text{otherwise.} \end{cases} \tag{2}$$

A. THz-Band Channel Model

1) Path Loss Model: In our proposed THz-band channel model, both the spreading loss and shadow fading characteristics of the transmission medium are considered as the main sources of signal attenuation. In the THz band, the path-loss is mainly characterized by the spreading loss and the molecular absorption loss [32]. The total path loss, denoted by $H_k(f, r_k)$, in the THz band for nano device k can be derived as follows [32]:

$$H_k(f, r_k) = H_{k,\text{spread}}(f, r_k) H_{k,\text{abs}}(r_k) \tag{3}$$

where $H_{k,\text{spread}}(f, r_k)$ and $H_{k,\text{abs}}(r_k)$ represent the spreading loss and molecular absorption attenuation, respectively, at transmission distance r_k and operating frequency f, which are defined as follows:

$$\begin{cases} H_{k,\text{spread}}(f, r_k) = \frac{c}{4\pi f r_k}; \\ H_{k,\text{abs}}(r_k) = \exp\left(-\frac{\alpha_{\text{abs}} r_k}{2}\right), \end{cases} \tag{4}$$

where c is the speed of light in free space and α_{abs} is the medium absorption coefficient, which depends on the molecular composition in the channel along the transmission path. Then, we can derive the received power, denoted by $\mathcal{P}_{\text{pathloss,r}}(r_k)$, at the nano receiver with the transmission distance r_k due to pathloss as follows:

$$\mathcal{P}_{\text{pathloss,r}}(r_k) = S(f) \left(\frac{c}{4\pi f r_k}\right)^2 e^{-\alpha_{\text{abs}} r_k} \tag{5}$$

where $S(f)$ is the power spectral density of the transmitted pulse. In addition, we can derive the received power, denoted by $\mathcal{P}_{\text{shadow,r}}(r_k)$, from nano transmitter k to its nano receiver with the transmission distance r_k due to shadowing as follows [38]:

$$\mathcal{P}_{\text{shadow,r}}(r_k) = (r_k)^{-\eta} G 10^{\frac{\xi_k}{10}} \tag{6}$$

where G denotes the channel gain constant, η is the path loss exponent, ξ_k is a random variable which represents the shadow fading characteristics of the transmission medium. Note that the parameters of the path-loss and shadowing models can be extracted based on empirical measurements or Monte Carlo simulations. According to the Central Limit Theorem, the shadow fading variable ξ_k can be considered as a normal distributed random variable with zero mean and standard deviation σ, i.e., $\xi_k \sim \mathcal{N}(0, \sigma^2)$. Then, we can derive the total received power, denoted by $\mathcal{P}_{\text{total}}(r_k)$, at the nano receiver across the transmission distance r_k from the nano transmitter k as follows:

$$\mathcal{P}_{\text{total}}(r_k) = (r_k)^{-\eta} G 10^{\frac{\xi_k}{10}} S(f) \left(\frac{c}{4\pi f r_k}\right)^2 e^{-\alpha_{\text{abs}} r_k}. \tag{7}$$

2) Noise Model: The noise in the THz band is mainly contributed by the molecular absorption noise, which is caused by vibrating molecules [32] [39]. The total power of the molecular absorption noise, denoted by $N_k(r_k)$, in the THz band is composed of the background noise, denoted by N_b, and the self-induced noise, denoted by $N_{k,s}(r_k)$, which is given as follows [40]:

$$N_k(r_k) = N_b + N_{k,s}(r_k) \tag{8}$$

where

$$\begin{cases} N_b = B(T_0, f) \left(\frac{c}{\sqrt{4\pi} f_0}\right)^2; \\ N_{k,s}(r_k) = S(f) \left(1 - e^{-\alpha_{\text{abs}} r_k}\right) \left(\frac{c}{4\pi f r_k}\right)^2, \end{cases} \tag{9}$$

where T_0 is the reference temperature of the medium, f_0 is the design centre frequency, and $B(T_0, f)$ is the Planck's function, which is given by [41]

$$B(T_0, f) = \frac{2h\pi f^3}{c^2} \left(e^{\frac{hf}{k_B T_0}} - 1\right)^{-1} \tag{10}$$

where k_B is the Boltzmann's constant and h is the Planck constant. We can observe from Eq. (9) that the background noise N_b depends on the temperature and composition of the medium. On the other hand, the self-induced noise $N_{k,s}(r_k)$ depends on the transmitted signal.

We define $\boldsymbol{x}_k^n \triangleq \left[x_k^{(1)}, \ldots, x_k^{(n)}\right]$ as the transmit signal vector from nano transmitter k, where n is the codeword blocklength. The transmit signal vector $\boldsymbol{x}_k^n$ is chosen randomly according to $\mathcal{N}(0, \overline{\mathcal{P}})$ with the following average power constraint:

$$\|\boldsymbol{x}_k^n\|^2 \leq \sqrt{n\overline{\mathcal{P}}} \tag{11}$$

where $\|\cdot\|^2$ denotes the Euclidean norm and $\overline{\mathcal{P}}$ is the average transmit power for the nano device. Define $\boldsymbol{y}_k^n \triangleq \left[y_k^{(1)}, \ldots, y_k^{(n)}\right]$ as the receive signal vector. Accordingly, we can derive the received signal, denoted by $\boldsymbol{y}_k^n$, for transmitting n data blocks from nano transmitter k to its nano receiver in the THz band in the finite blocklength regime as follows:

$$\boldsymbol{y}_k^n = \sqrt{\mathcal{P}_{\text{total}}(r_k)} \boldsymbol{x}_k^n + \sum_{i=1, i\neq k}^{K+1} \sqrt{\mathcal{P}_{\text{total}}(r_i)} \boldsymbol{x}_i^n + \boldsymbol{n}_k \tag{12}$$

where $\mathcal{P}_{\text{total}}(r_k)$ and $\mathcal{P}_{\text{total}}(r_i)$ are the received signal powers at the nano receiver across the transmission distances r_k and

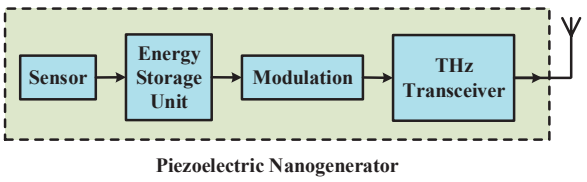

Fig. 2. The piezoelectric nanogenerator model in the THz band.

r_i from nano transmitters k and i, respectively, as specified by Eq. (7), $\boldsymbol{x}_k^n$ and $\boldsymbol{x}_i^n$ represent the transmitted signal from nano transmitter k and i, respectively, r_i is the transmission distance from the nano transmitter i to its assigned nano receiver, and $\boldsymbol{n}_k$ denotes the absorption noise with power given by Eq. (8).

B. EH Model for Piezoelectric Nanogenerators

Recently, researchers have developed the piezoelectric nanogenerators [42] [43] for converting mechanical energy into electrical energy, as shown in Fig. 2. Due to the low energy consumption of nano devices over a short distance in the THz band, the energy harvested from the environment should be sufficient to power the nano devices. Without loss of generality, we assume that all harvested energy can be stored in the nanocapacitor. We can derive the stored energy, denoted by E_{cap}, in the nanocapacitor after a number of cycles, denoted by n_{cyc}, as follows [44]:

$$E_{\text{cap}}(n_{\text{cyc}}) = \frac{1}{2} C_{\text{cap}} \left[V_{\text{cap}}(n_{\text{cyc}})\right]^2 \tag{13}$$

where C_{cap} and $V_{\text{cap}}(n_{\text{cyc}})$ are the total capacitance and voltage function of the nano-capacitor, respectively. Then, the voltage function $V_{\text{cap}}(n_{\text{cyc}})$ of the charging nanocapacitor can be derived as follows:

$$\begin{aligned} V_{\text{cap}}(n_{\text{cyc}}) &= V_g \left[1 - \exp\left(-\frac{n_{\text{cyc}} t_{\text{cyc}}}{R_g C_{\text{cap}}}\right)\right] \\ &= V_g \left[1 - \exp\left(-\frac{n_{\text{cyc}} \Delta Q}{V_g C_{\text{cap}}}\right)\right] \end{aligned} \tag{14}$$

where V_g represents the generator voltage, R_g is the resistor, t_{cyc} is the time between consecutive cycles, and ΔQ is the amount of electric charge obtained from one cycle. We can derive the maximum energy, denoted by $E_{\text{cap}}^{\max}(n_{\text{cyc}})$, stored in the nanocapacitor as follows:

$$E_{\text{cap}}^{\max}(n_{\text{cyc}}) = \frac{1}{2} C_{\text{cap}} \left(V_g\right)^2. \tag{15}$$

Furthermore, the energy harvesting rate, denoted by λ_{eh}, in Joule/second can be computed as a function of the current energy $E_{\text{cap}}(n_{\text{cyc}})$ in the nano-capacitor and the increment in the energy of the nano-capacitor, denoted by ΔE, which is given as follows [45]:

$$\lambda_{\text{eh}} = \frac{V_g \Delta Q}{t_{\text{cyc}}} \left[\exp\left(-\frac{\Delta Q n_{\text{cyc}}}{V_g C_{\text{cap}}}\right) - \exp\left(-\frac{2\Delta Q n_{\text{cyc}}}{V_g C_{\text{cap}}}\right)\right]. \tag{16}$$

C. Channel Coding Rate in the Finite Blocklength Regime

Definition 1. The (n, M, ϵ_k)-Code. We define a message set $\mathcal{M} = \{1, \ldots, M\}$ and a message m is uniformly distributed on $\mathcal{M}$, where M is the total number of codewords and ϵ_k is the decoding error probability. Correspondingly, we define an (n, M, ϵ_k)-code as follows:

- An encoder Υ: $\{1, \ldots, M\} \mapsto \mathcal{A}^n$ that maps the message $m \in \{1, \ldots, M\}$ into a codeword, denoted by $\boldsymbol{x}_{\boldsymbol{k}}^{\boldsymbol{n}}$, with length n, where $\mathcal{A}^n$ is the codebook which represents the set of all the possible codewords mapped by the encoding function Υ.
- A decoder $\mathcal{D}$: $\mathcal{B}^n \mapsto \{1, \ldots, M\}$ that decodes the received message into $\widehat{m}$, where $\mathcal{B}^n$ is the set of received codewords of length n and $\widehat{m}$ denotes the estimated signal received at the receiver. The decoder $\mathcal{D}$ need to satisfy the following maximum error probability constraint:

$$\Pr\{\widehat{m} \neq m\} \leq \epsilon_k. \tag{17}$$

We define $Q_{Y_k^n}$ as an arbitrary distribution on the output alphabet. Define the modified information density, denoted by $\boldsymbol{i}(\boldsymbol{x}_k^n; \boldsymbol{y}_k^n)$, for nano transmitter (device) k as follows [46]:

$$\boldsymbol{i}(\boldsymbol{x}_k^n; \boldsymbol{y}_k^n) \triangleq \frac{1}{n} \log_2 \left[\frac{P_{Y_k^n|X_k^n}(\boldsymbol{y}_k^n|\boldsymbol{x}_k^n)}{Q_{Y_k^n}(y_k^n)}\right] \tag{18}$$

where $P_{Y_k^n|X_k^n}$ denotes the conditional probability distribution function.

Definition 2. The Channel Coding Rate. In [12], the maximum achievable coding rate, denoted by $R(n, r_k, \mathcal{P}_k)$, (in bits per channel use) with error probability ϵ_k $(0 \leq \epsilon_k < 1)$, transmitted power, denoted by $\mathcal{P}_k$, and coding blocklength n for nano transmitter k in the finite blocklength regime can be determined as follows [12]:

$$R(n, r_k, \mathcal{P}_k) = C(r_k, \mathcal{P}_k) - \sqrt{\frac{V(r_k, \mathcal{P}_k)}{n}} Q^{-1}(\epsilon_k) + \frac{\mathcal{O}(\log n)}{n} \tag{19}$$

where $Q^{-1}(\cdot)$ is the inverse of Q-function, $\mathcal{O}(\cdot)$ is the big O notation so that $\mathcal{O}(\log n)/n$ is negligible when n gets large, and $C(r_k, \mathcal{P}_k)$ and $V(r_k, \mathcal{P}_k)$ are the channel capacity and channel dispersion, respectively. Eq. (19) implies that, given a codeword with finite length n, the achievable coding rate can be derived by the right-hand side of Eq. (19) with decoding error probability no larger than ϵ_k.

III. The THz-Band Wireless Channel Modeling in the Finite Blocklength Regime

In this section, we characterize the functions of aggregate interference, channel capacity, channel dispersion, and the ϵ-effective capacity, respectively, in supporting mURLLC over FBC-EH based 6G THz wireless nano-networks.

A. The Aggregate Interference Modeling for the THz-Band Channels

Using Eqs. (7) and (8), we can derive the signal to interference and noise ratio (SINR) function, denoted by $\gamma_k^{(l)}(\boldsymbol{r})$ $(l = 1, \ldots, n)$, between nano transmitter k and its nano

receiver for transmitting the lth data block in the THz band as follows:

$$\gamma_k^{(l)}(\boldsymbol{r}) = \frac{\mathcal{P}_k \mathcal{P}_{\text{total}}(r_k)}{N_{I_k^{(l)}}(\boldsymbol{r}) + N_k(r_k)} \tag{20}$$

where $\boldsymbol{r}$ represents the vector of distances r_k $(k = 1, 2, \ldots, (K+1))$ between nano transmitter k and its nano receiver, $N_{I_k^{(l)}}(\boldsymbol{r})$ is the aggregate interference power, and $N_k(r_k)$ is the noise power. To guarantee the successful reception of the transmitted symbol at the nano receiver, the received SINR should be larger than a threshold, denoted by γ_{th}, i.e., $\gamma_k^{(l)}(\boldsymbol{r}) \geq \gamma_{\text{th}}$. We have

$$\frac{\mathcal{P}_k \left(r_k\right)^{-\eta} G 10^{\frac{\xi_k}{10}} S(f) \left(\frac{c}{4\pi f r_k}\right)^2 e^{-\alpha_{\text{abs}} r_k}}{N_k(r_k) + N_{I_k^{(l)}}(\boldsymbol{r})} \geq \gamma_{\text{th}}. \tag{21}$$

We can derive the aggregate interference, denoted by $I_k^{(l)}(\boldsymbol{r})$, at the nano receiver for transmitting the lth data block in the THz band as follows:

$$I_k^{(l)}(\boldsymbol{r}) = \sum_{i=1, i\neq k}^{K+1} \sqrt{\mathcal{P}_i \left(r_i\right)^{-\eta} G 10^{\frac{\xi_i}{10}} S(f)} \left(\frac{c}{4\pi f r_i}\right) e^{-\frac{\alpha_{\text{abs}} r_i}{2}} + N_i(r_i). \tag{22}$$

Due to the high density of wireless nano-networks, i.e., as $K \to \infty$, we can invoke the Central Limit Theorem and assume that the aggregate interference can be modeled as a Gaussian random process, i.e., $I_k^{(l)}(\boldsymbol{r}) \sim \mathcal{N}\left(\mathbb{E}_{\boldsymbol{r}}[I_k^{(l)}(\boldsymbol{r})], \text{Var}_{I_k^{(l)}}(\boldsymbol{r})\right)$, where $\mathbb{E}_{\boldsymbol{r}}[I_k^{(l)}(\boldsymbol{r})]$ and $\text{Var}_{I_k^{(l)}}(\boldsymbol{r})$ are the mean and variance of the aggregate interference, respectively, and $\mathbb{E}_{\boldsymbol{r}}[\cdot]$ is the expectation operation with respect to $\boldsymbol{r}$. We derive the closed-form expressions for characterizing the mean $\mathbb{E}_{\boldsymbol{r}}[I_k^{(l)}(\boldsymbol{r})]$ and the variance $\text{Var}_{I_k^{(l)}}(\boldsymbol{r})$, respectively, of the aggregate interference in the following theorem.

Theorem 1: **If** the aggregate interference $I_k^{(l)}(\boldsymbol{r})$ is given by Eq. (22) for our proposed THz-band channel model, **then** the *mean* and *variance* of the aggregate interference between nano transmitter k and its nano receiver in the THz band over wireless nano-networks are characterized by the following two claims, respectively:

Claim 1: The *mean* $\mathbb{E}_{\boldsymbol{r}}[I_k^{(l)}(\boldsymbol{r})]$ of the aggregate interference is accurately estimated by its lower-bound as follows:

$$\mathbb{E}_{\boldsymbol{r}}[I_k^{(l)}(\boldsymbol{r})] \geq \frac{2\lambda\pi a^2 \Lambda \sqrt{\overline{\mathcal{P}}} \left(\frac{2}{\alpha_{\text{abs}}}\right)^{1-\frac{\eta}{2}}}{a^2 - b^2} \left[\gamma\left(1 - \frac{\eta}{2}, \frac{\alpha_{\text{abs}} a}{2}\right) - \gamma\left(1 - \frac{\eta}{2}, \frac{\alpha_{\text{abs}} b}{2}\right)\right] \tag{23}$$

where $\gamma(\cdot, \cdot)$ is the lower incomplete Gamma function and

$$\Lambda \triangleq \frac{c\sqrt{GS(f)}}{4\pi f}. \tag{24}$$

Claim 2: The *variance* $\text{Var}_{I_k^{(l)}}(\boldsymbol{r})$ of the aggregate interference is approximated as follows:

$$\text{Var}_{I_k^{(l)}}(\boldsymbol{r}) \approx \frac{6\lambda\pi a^2 \Lambda^2 \overline{\mathcal{P}} (\alpha_{\text{abs}})^{-\eta}}{a^2 - b^2} [\gamma(-\eta, a\alpha_{\text{abs}}) - \gamma(-\eta, b\alpha_{\text{abs}})] + \sum_{i=1, i\neq k}^{K+1} N_{i,b} + \frac{2\lambda\pi a^2 \Lambda^2}{a^2 - b^2} \left[\log\left(\frac{a}{b}\right) - \text{Ei}\left(-\alpha_{\text{abs}} a\right) + \text{Ei}\left(-\alpha_{\text{abs}} b\right)\right] - \left(\frac{2\lambda\pi a^2 C}{a^2 - b^2}\right)^2 \overline{\mathcal{P}} \left(\frac{2}{\alpha_{\text{abs}}}\right)^{2-\eta} \times \left[\gamma\left(1 - \frac{\eta}{2}, \frac{\alpha_{\text{abs}} a}{2}\right) - \gamma\left(1 - \frac{\eta}{2}, \frac{\alpha_{\text{abs}} b}{2}\right)\right]^2. \tag{25}$$

Proof: To derive the closed-form expressions for the mean and variance of the aggregate interference, we prove **Claim 1** and **Claim 2**, respectively, for this theorem as follows.

Claim 1: We can derive the mean of aggregate interference $\mathbb{E}_{\boldsymbol{r}}[I_k^{(l)}(\boldsymbol{r})]$ between nano node k and its nano receiver in the THz band over wireless nano-networks as follows:

$$\mathbb{E}_{\boldsymbol{r}}[I_k^{(l)}(\boldsymbol{r})] = \mathbb{E}_{\boldsymbol{r}}\left[\sum_{i=1, i\neq k}^{K+1} \sqrt{\mathcal{P}_i \mathcal{P}_{\text{total}}(r_i)}\right]. \tag{26}$$

Then, in order to calculate the mean of aggregate interference $\mathbb{E}_{\boldsymbol{r}}[I_k^{(l)}(\boldsymbol{r})]$, first we need to calculate the expression function given in the right-hand-side of Eq. (26) as follows:

$$\begin{aligned}
&\mathbb{E}_{\boldsymbol{r}}\left[\sum_{i=1, i\neq k}^{K+1} \sqrt{\mathcal{P}_i \mathcal{P}_{\text{total}}(r_i)}\right] \\
&= \mathbb{E}_{\boldsymbol{r}}\left[\sum_{i=1, i\neq k}^{K+1} \sqrt{\mathcal{P}_i \left(r_i\right)^{-\eta} G 10^{\frac{\xi_i}{10}} S(f)} \left(\frac{c}{4\pi f r_i}\right) e^{-\frac{\alpha_{\text{abs}} r_i}{2}}\right] \\
&= \Lambda \mathbb{E}_{\boldsymbol{r}}\left[\sum_{i=1, i\neq k}^{K+1} \sqrt{\mathcal{P}_i 10^{\frac{\xi_i}{10}}} F(r_i)\right]
\end{aligned} \tag{27}$$

where Λ is given by Eq. (24) and

$$F(r_i) \triangleq r_i^{-\frac{\eta}{2}-1} e^{-\frac{\alpha_{\text{abs}} r_i}{2}}. \tag{28}$$

Then, we need to calculate the function $\mathbb{E}_{\boldsymbol{r}}\left[\sum_{i=1, i\neq k}^{K+1} \sqrt{\mathcal{P}_i 10^{\frac{\xi_i}{10}}} F(r_i)\right]$. Assuming that random number $\mathcal{K}$ interfering nano nodes (transmitters) is equal to κ, we can obtain the conditional expectation function as follows [47]:

$$\begin{aligned}
&\mathbb{E}_{\boldsymbol{r}}\left[\sum_{i=1, i\neq k}^{K+1} \sqrt{\mathcal{P}_i 10^{\frac{\xi_i}{10}}} F(r_i) \middle| \mathcal{K} = \kappa\right] \\
&= \sum_{i=1, i\neq k}^{K+1} \mathbb{E}_{\boldsymbol{r}}\left[\sqrt{\mathcal{P}_i 10^{\frac{\xi_i}{10}}} F(r_i) \middle| \mathcal{K} = \kappa\right] = \kappa \mathbb{E}_{r_i}\left[\sqrt{\mathcal{P}_i 10^{\frac{\xi_i}{10}}} F(r_i)\right] \\
&\geq \kappa \mathbb{E}_{r_i}\left[\sqrt{\mathcal{P}_i 10^{\frac{\xi_i}{10}}}\right] \mathbb{E}_{r_i}[F(r_i)] = \kappa \sqrt{\overline{\mathcal{P}}} \mathbb{E}_{r_i}\left[F(r_i)\right]
\end{aligned} \tag{29}$$

where $\mathbb{E}_{r_i}[\cdot]$ is the expectation operation with respect to r_i and

$$\begin{aligned}
\mathbb{E}_{r_i}[F(r_i)] &= \int_b^a r_i^{-\frac{\eta}{2}-1} e^{-\frac{\alpha_{\text{abs}} r_i}{2}} f_D(r_i) dr_i \\
&= \frac{2}{a^2 - b^2} \int_b^a r_i^{-\frac{\eta}{2}} e^{-\frac{\alpha_{\text{abs}} r_i}{2}} dr_i
\end{aligned}$$

$$= \frac{2\left(\frac{2}{\alpha_{\text{abs}}}\right)^{1-\frac{\eta}{2}}}{a^2-b^2} \int_{\frac{\alpha_{\text{abs}} b}{2}}^{\frac{\alpha_{\text{abs}} a}{2}} r_i^{-\frac{\eta}{2}} e^{-r_i} dr_i$$
$$= \frac{2\left(\frac{2}{\alpha_{\text{abs}}}\right)^{1-\frac{\eta}{2}}}{a^2-b^2} \left[\gamma\left(1-\frac{\eta}{2}, \frac{\alpha_{\text{abs}} a}{2}\right) - \gamma\left(1-\frac{\eta}{2}, \frac{\alpha_{\text{abs}} b}{2}\right)\right]. \quad (30)$$

In addition, using the spatial Poisson process, we can obtain the mean and variance of the number of interfering nano nodes $\mathcal{K}$ as follows:

$$\begin{cases} \mathbb{E}[\mathcal{K}] = \lambda \pi a^2; \\ \text{Var}(\mathcal{K}) = \lambda \pi a^2, \end{cases} \quad (31)$$

where $\mathbb{E}[\cdot]$ and $\text{Var}(\cdot)$ are the standard expectation and variance operations, respectively. Correspondingly, using Eqs. (30) and (31), we can obtain the following equation:

$$\mathbb{E}_{\boldsymbol{r}}\left[\sum_{i=1, i\neq k}^{K+1} \sqrt{\mathcal{P}_i 10^{\frac{\xi_i}{10}}} F(r_i)\right] \geq \mathbb{E}\left[\mathcal{K}\right] \sqrt{\overline{\mathcal{P}}} \mathbb{E}_{r_i}\left[F(r_i)\right]$$
$$= \frac{2\lambda\pi a^2 \sqrt{\overline{\mathcal{P}}} \left(\frac{2}{\alpha_{\text{abs}}}\right)^{1-\frac{\eta}{2}}}{a^2-b^2} \left[\gamma\left(1-\frac{\eta}{2}, \frac{\alpha_{\text{abs}} a}{2}\right) - \gamma\left(1-\frac{\eta}{2}, \frac{\alpha_{\text{abs}} b}{2}\right)\right]. \quad (32)$$

As a result, by plugging Eq. (32) back into Eq. (27), we can characterize the mean of aggregate interference $\mathbb{E}_{\boldsymbol{r}}[I_k^{(l)}(\boldsymbol{r})]$ as follows:

$$\mathbb{E}_{\boldsymbol{r}}[I_k^{(l)}(\boldsymbol{r})] \geq \frac{2\lambda\pi a^2 \Lambda \sqrt{\overline{\mathcal{P}}} \left(\frac{2}{\alpha_{\text{abs}}}\right)^{1-\frac{\eta}{2}}}{a^2-b^2} \left[\gamma\left(1-\frac{\eta}{2}, \frac{\alpha_{\text{abs}} a}{2}\right) - \gamma\left(1-\frac{\eta}{2}, \frac{\alpha_{\text{abs}} b}{2}\right)\right] \quad (33)$$

which is Eq. (23). Thus, we complete the proof for **Claim 1** in Theorem 1.

Claim 2: We can derive the variance of the aggregate interference $\text{Var}_{I_k^{(l)}}(\boldsymbol{r})$ for our proposed THz-band nano-communication schemes as follows:

$$\text{Var}_{I_k^{(l)}}(\boldsymbol{r}) = \mathbb{E}_{\boldsymbol{r}}\left[\left(I_k^{(l)}(\boldsymbol{r})\right)^2\right] - \left(\mathbb{E}_{\boldsymbol{r}}[I_k^{(l)}(\boldsymbol{r})]\right)^2 \quad (34)$$

where

$$\mathbb{E}_{\boldsymbol{r}}\left[\left(I_k^{(l)}(\boldsymbol{r})\right)^2\right] = \mathbb{E}_{\boldsymbol{r}}\left[\sum_{i=1, i\neq k}^{K+1} \mathcal{P}_i \mathcal{P}_{\text{total}}(r_i) + N_i(r_i)\right] + 2\mathbb{E}_{\boldsymbol{r}}\left[\sum_{i=1, i\neq k}^{K+1} \sum_{j=1}^{i-1} \sqrt{\mathcal{P}_i \mathcal{P}_j \mathcal{P}_{\text{total}}(r_i) \mathcal{P}_{\text{total}}(r_j)}\right]. \quad (35)$$

To obtain the variance of aggregate interference by $\text{Var}_{I_k^{(l)}}(\boldsymbol{r})$, first we need to obtain the following equation:

$$\mathbb{E}_{\boldsymbol{r}}\left[\sum_{i=1, i\neq k}^{K+1} \mathcal{P}_i \mathcal{P}_{\text{total}}(r_i)\right] = \mathbb{E}_{\boldsymbol{r}}\left[\sum_{i=1, i\neq k}^{K+1} \mathcal{P}_i \left(r_i\right)^{-\eta} G 10^{\frac{\xi_i}{10}} S(f) \times \left(\frac{c}{4\pi f r_i}\right)^2 e^{-\alpha_{\text{abs}} r_i}\right]$$
$$= \Lambda^2 \mathbb{E}_{\boldsymbol{r}}\left[\sum_{i=1, i\neq k}^{K+1} \mathcal{P}_i 10^{\frac{\xi_i}{10}} \widetilde{F}(r_i)\right] \quad (36)$$

where

$$\widetilde{F}(r_i) \triangleq (r_i)^{-\eta-2} e^{-\alpha_{\text{abs}} r_i}. \quad (37)$$

Since the transmission power $\mathcal{P}_i$ is upper-bounded by $\overline{\mathcal{P}}$, we can then obtain the conditional expectation function as follows:

$$\mathbb{E}_{\boldsymbol{r}}\left[\sum_{i=1, i\neq k}^{K+1} \mathcal{P}_i 10^{\frac{\xi_i}{10}} \widetilde{F}(r_i) \middle| \mathcal{K} = \kappa\right] = \kappa \mathbb{E}_{r_i}\left[\mathcal{P}_i 10^{\frac{\xi_i}{10}} \widetilde{F}(r_i)\right]$$
$$\geq \kappa \mathbb{E}_{r_i}\left[\mathcal{P}_i 10^{\frac{\xi_i}{10}}\right] \mathbb{E}_{r_i}\left[\widetilde{F}(r_i)\right] = \kappa \overline{\mathcal{P}} \mathbb{E}_{r_i}\left[\widetilde{F}(r_i)\right] \quad (38)$$

where

$$\mathbb{E}_{r_i}\left[\widetilde{F}(r_i)\right] = \int_b^a (r_i)^{-\eta-2} e^{-\alpha_{\text{abs}} r_i} f_D(r_i) dr_i$$
$$= \frac{2}{a^2-b^2} \int_b^a (r_i)^{-\eta-1} e^{-\alpha_{\text{abs}} r_i} dr_i$$
$$= \frac{2(\alpha_{\text{abs}})^{-\eta}}{a^2-b^2} \int_{b\alpha_{\text{abs}}}^{a\alpha_{\text{abs}}} (r_i)^{-\eta-1} e^{-r_i} dr_i$$
$$= \frac{2(\alpha_{\text{abs}})^{-\eta}}{a^2-b^2} \left[\gamma\left(-\eta, a\alpha_{\text{abs}}\right) - \gamma\left(-\eta, b\alpha_{\text{abs}}\right)\right]. \quad (39)$$

Using Eqs. (31), (36), and (39), we can obtain the following inequation:

$$\mathbb{E}_{\boldsymbol{r}}\left[\sum_{i=1, i\neq k}^{K+1} \mathcal{P}_i \mathcal{P}_{\text{total}}(r_i)\right] \geq \frac{2\lambda\pi a^2 \Lambda^2 \overline{\mathcal{P}} (\alpha_{\text{abs}})^{-\eta}}{a^2-b^2} \times \left[\gamma\left(-\eta, a\alpha_{\text{abs}}\right) - \gamma\left(-\eta, b\alpha_{\text{abs}}\right)\right]. \quad (40)$$

We also need to show that the following equations hold true:

$$\mathbb{E}_{\boldsymbol{r}}\left[\sum_{i=1, i\neq k}^{K+1} N_i(r_i)\right] = \mathbb{E}_{\boldsymbol{r}}\left[\sum_{i=1, i\neq k}^{K+1} \left(N_{i,b} + N_{i,s}(r_i)\right)\right]$$
$$= \sum_{i=1, i\neq k}^{K+1} N_{i,b} + \mathbb{E}_{\boldsymbol{r}}\left[\sum_{i=1, i\neq k}^{K+1} N_{i,s}(r_i)\right]$$
$$= \sum_{i=1, i\neq k}^{K+1} N_{i,b} + \mathbb{E}_{\boldsymbol{r}}\left[\sum_{i=1, i\neq k}^{K+1} S(f)\left(1-e^{-\alpha_{\text{abs}} r_i}\right)\left(\frac{c}{4\pi f r_i}\right)^2\right]$$
$$= \sum_{i=1, i\neq k}^{K+1} N_{i,b} + \Lambda^2 \mathbb{E}_{\boldsymbol{r}}\left[\sum_{i=1, i\neq k}^{K+1} \widehat{F}(r_i)\right] \quad (41)$$

where

$$\widehat{F}(r_i) \triangleq (r_i)^{-2}\left(1 - e^{-\alpha_{\text{abs}} r_i}\right). \quad (42)$$

Similarly, we can obtain the conditional expectation function as follows:

$$\mathbb{E}_{\boldsymbol{r}|\mathcal{K}}\left[\sum_{i=1, i\neq k}^{K+1} \widehat{F}(r_i) \middle| \mathcal{K} = \kappa\right] = \kappa \mathbb{E}_{r_i}\left[\widehat{F}(r_i)\right] \quad (43)$$

where $\mathbb{E}_{\boldsymbol{r}|\mathcal{K}}[\cdot]$ represents conditional expectation operations and

$$\begin{aligned}\mathbb{E}_{r_i}\left[\widehat{F}(r_i)\right] &= \int_b^a (r_i)^{-2}\left(1-e^{-\alpha_{\text{abs}}r_i}\right) f_D(r_i)dr_i \\ &= \frac{2}{a^2-b^2}\int_b^a \frac{1-e^{-\alpha_{\text{abs}}r_i}}{r_i}dr_i \\ &= \frac{2}{a^2-b^2}\left[\log\left(\frac{a}{b}\right) - \text{Ei}\left(-\alpha_{\text{abs}}a\right) + \text{Ei}\left(-\alpha_{\text{abs}}b\right)\right]\end{aligned} \tag{44}$$

where $\log(\cdot)$ represents $\log_e(\cdot)$ and $\text{Ei}(x)$ is the exponential integral function, which is defined as follows:

$$\text{Ei}(x) \triangleq -\int_{-x}^{\infty}\frac{e^{-t}}{t}dt. \tag{45}$$

Similar to Eq. (40), we can obtain the following equation:

$$\begin{aligned}\mathbb{E}_{\boldsymbol{r}}\left[\sum_{i=1,i\neq k}^{K+1}\widehat{F}(r_i)\right] = \frac{2\lambda\pi a^2}{a^2-b^2}\Bigg[\log\left(\frac{a}{b}\right) - \text{Ei}\left(-\alpha_{\text{abs}}a\right) \\ + \text{Ei}\left(-\alpha_{\text{abs}}b\right)\Bigg].\end{aligned} \tag{46}$$

Furthermore, due to the high density of wireless nano-networks, we assume that the distances r_i $(i = 1, \ldots, K+1$ and $i \neq k)$ between its nano receiver and all interfering nano nodes are approximately the same. As a result, we get

$$\begin{aligned}&\mathbb{E}_{\boldsymbol{r}}\left[\sum_{i=1,i\neq k}^{K+1}\sum_{j=1}^{i-1}\sqrt{\mathcal{P}_i\mathcal{P}_j\mathcal{P}_{\text{total}}(r_i)\mathcal{P}_{\text{total}}(r_j)}\right] \\ &\geq \Lambda^2\mathbb{E}\left[\mathcal{K}\right]\mathbb{E}_{r_i}\left[\mathcal{P}_i 10^{\frac{\xi_i}{10}}\widetilde{F}(r_i)\right] \\ &\geq \frac{2\lambda\pi a^2\Lambda^2\overline{\mathcal{P}}(\alpha_{\text{abs}})^{-\eta}}{a^2-b^2}\left[\gamma\left(-\eta, a\alpha_{\text{abs}}\right) - \gamma\left(-\eta, b\alpha_{\text{abs}}\right)\right].\end{aligned} \tag{47}$$

Therefore, plugging Eqs. (40) and (47) back into Eq. (35), we can obtain the following equation:

$$\begin{aligned}\mathbb{E}_{\boldsymbol{r}}\left[\left(I_k^{(l)}(\boldsymbol{r})\right)^2\right] \approx \frac{6\lambda\pi a^2\Lambda^2\overline{\mathcal{P}}(\alpha_{\text{abs}})^{-\eta}}{a^2-b^2}\big[\gamma\left(-\eta, a\alpha_{\text{abs}}\right) \\ - \gamma\left(-\eta, b\alpha_{\text{abs}}\right)\big] + \sum_{i=1,i\neq k}^{K+1}N_{i,b} + \frac{2\lambda\pi a^2\Lambda^2}{a^2-b^2} \\ \times\left[\log\left(\frac{a}{b}\right) - \text{Ei}\left(-\alpha_{\text{abs}}a\right) + \text{Ei}\left(-\alpha_{\text{abs}}b\right)\right].\end{aligned} \tag{48}$$

Consequently, substituting Eq. (48) back into Eq. (34), we can derive the approximate variance of aggregate interference $\text{Var}_{I_k^{(l)}}(\boldsymbol{r})$ as follows:

$$\begin{aligned}\text{Var}_{I_k^{(l)}}(\boldsymbol{r}) \approx \frac{6\lambda\pi a^2\Lambda^2\overline{\mathcal{P}}(\alpha_{\text{abs}})^{-\eta}}{a^2-b^2}\left[\gamma(-\eta, a\alpha_{\text{abs}}) - \gamma(-\eta, b\alpha_{\text{abs}})\right] \\ + \sum_{i=1,i\neq k}^{K+1}N_{i,b} + \frac{2\lambda\pi a^2\Lambda^2}{a^2-b^2}\Bigg[\log\left(\frac{a}{b}\right) - \text{Ei}\left(-\alpha_{\text{abs}}a\right) \\ + \text{Ei}\left(-\alpha_{\text{abs}}b\right)\Bigg] - \left(\frac{2\lambda\pi a^2 C}{a^2-b^2}\right)^2\overline{\mathcal{P}}\left(\frac{2}{\alpha_{\text{abs}}}\right)^{2-\eta} \\ \times\left[\gamma\left(1-\frac{\eta}{2}, \frac{\alpha_{\text{abs}}a}{2}\right) - \gamma\left(1-\frac{\eta}{2}, \frac{\alpha_{\text{abs}}b}{2}\right)\right]^2\end{aligned} \tag{49}$$

which is Eq. (25). Thus, we complete the proof for **Claim 2** in Theorem 1. ■

Remarks on Theorem 1: The expressions derived in Theorem 1 for the *mean* and *variance* of the aggregate interference play the important roles in modeling the *channel capacity* and *channel dispersion*, which are to be investigated in Section III-C and Section III-D, respectively, over our proposed THz-band wireless nano-networks.

B. The ϵ-Effective Capacity in the Finite Blocklength Regime

Statistical delay-bounded QoS guarantees [3] have been extensively studied for analyzing queuing behavior for time-varying arrival and service processes. Traditionally, the effective capacity measures queuing process which is independent of the decoding error at the receiver. Based on the Large Deviation Principle (LDP) [48], under sufficient conditions, the queueing process $Q_k(t)$ converges in distribution to a random variable $Q_k(\infty)$ such that

$$-\lim_{Q_{\text{th},k}\to\infty}\frac{\log\left(\Pr\left\{Q_k(\infty) > Q_{\text{th},k}\right\}\right)}{Q_{\text{th},k}} = \theta_k \tag{50}$$

where $Q_{\text{th},k}$ represents the overflow threshold at the nano device k and $\theta_k > 0$ is defined as the *QoS exponent* for the nano device k. To be more specific, Eq. (50) states that the probability of the queuing process exceeding a certain threshold $Q_{\text{th},k}$ decays exponentially fast as the threshold $Q_{\text{th},k}$ increases. As shown in [49], a smaller θ_k corresponds to a slower decay rate, which implies that the system can only provide a looser QoS guarantee, while a larger θ_k leads to a faster decay rate, which means that a more stringent QoS can be supported. In particular, when $\theta_k \to 0$, the system can tolerate an arbitrarily long delay; when $\theta_k \to \infty$, the system cannot tolerate any delay.

For our proposed FBC-EH based 6G THz wireless communication schemes, we need to consider both delay and error-rate bounded QoS requirements. Thus, we introduce the new concept of ϵ-effective capacity as follows.

Definition 3. The ϵ-Effective Capacity. For an (n, M, ϵ_k)-code, given a desired decoding error probability ϵ_k and QoS exponent θ_k, the *ϵ-effective capacity*, denoted by $EC_\epsilon(\theta_k)$, between the nano transmitter k and its nano receiver within the THz-band covered region is defined as the maximum constant arrival rate for a given service process and decoding error probability in supporting our proposed statistical delay and error-rate bounded QoS provisioning in the finite blocklength regime is given as follows:

$$EC_\epsilon(\theta_k) \triangleq -\frac{1}{\theta_k}\log\left\{\mathbb{E}_{r_k}\left[\epsilon_k + (1-\epsilon_k)\,e^{-\theta_k n R(n, r_k, \mathcal{P}_k)}\right]\right\} \tag{51}$$

where $\mathbb{E}_{r_k}[\cdot]$ denotes expectation with respect to the random variable of transmission distance r_k between the nano transmitter k and its nano receiver within the THz-band covered region and $R(n, r_k, \mathcal{P}_k)$ is the maximum achievable coding

rate specified by Eq. (19). To derive the ϵ-effective capacity $EC_{\epsilon}(\theta_k)$, we need to derive the closed-form expressions for characterizing both *channel capacity* $C(r_k, \mathcal{P}_k)$ and *channel dispersion* $V(r_k, \mathcal{P}_k)$, which are elaborated on in the following two sections, respectively.

C. The Channel Capacity Modeling Over the THz Band in the Finite Blocklength Regime

Leveraging the Shannon Limit Theorem, we can derive the *channel capacity* $C(r_k, \mathcal{P}_k)$ in terms of the mutual information $I(\boldsymbol{x}_k^n, \boldsymbol{y}_k^n)$ for our proposed statistical delay and error-rate bounded QoS provisioning in supporting mURLLC over FBC-EH based 6G THz wireless nano-networks as follows:

$$C(r_k, \mathcal{P}_k) = \sup_{P_{X_k^n}(\boldsymbol{x}_k^n)} \{I(\boldsymbol{x}_k^n, \boldsymbol{y}_k^n)\} \tag{52}$$

where $P_{X_k^n}(\boldsymbol{x}_k^n)$ is the input symbol probability and $I(\boldsymbol{x}_k^n, \boldsymbol{y}_k^n)$ is the *mutual information*, which is given as follows:

$$I(\boldsymbol{x}_k^n, \boldsymbol{y}_k^n) = \mathbb{E}\left[\boldsymbol{i}(\boldsymbol{x}_k^n; \boldsymbol{y}_k^n)\right] = \frac{1}{n}\mathbb{E}\left[\log_2\left(\frac{P_{Y_k^n|X_k^n}(\boldsymbol{y}_k^n|\boldsymbol{x}_k^n)}{Q_{Y_k^n}(\boldsymbol{y}_k^n)}\right)\right] \tag{53}$$

where $\mathbb{E}[\cdot]$ is the expectation operation over the transmit and receive signals. The theorem that follows bellow derives the closed-form expression for the upper-bound to accurately approximate the channel capacity $C(r_k, \mathcal{P}_k)$ given by Eq. (52) over the THz band in the finite blocklength regime.

Theorem 2: The upper-bound on the *mutual information* $I(\boldsymbol{x}_k^n, \boldsymbol{y}_k^n)$ given by Eq. (53) for our proposed statistical delay and error-rate bounded QoS provisioning in supporting mURLLC over FBC-EH based 6G THz wireless nano-networks is given as follows:

$$I(\boldsymbol{x}_k^n, \boldsymbol{y}_k^n) \leq \frac{1}{2}\log_2\left[\frac{\mathcal{P}_k\mathcal{P}_{\text{total}}(r_k) + N_{I_k^{(l)}}(\boldsymbol{r}) + N_k(r_k)}{N_{I_k^{(l)}}(\boldsymbol{r}) + N_k(r_k)}\right] - (\log_2 e)\left[\frac{\mathcal{P}_k\left[\mathcal{P}_{\text{total}}(r_k) + 1\right]}{N_{I_k^{(l)}}(\boldsymbol{r}) + N_k(r_k)}\right]. \tag{54}$$

Proof: To derive the upper-bound given by Eq. (54) on the mutual information $I(\boldsymbol{x}_k^n, \boldsymbol{y}_k^n)$ given by Eq. (53) to accurately approximate the channel capacity $C(r_k, \mathcal{P}_k)$ given by Eq. (52), we need to proceed with the following four steps.

Step 1: We need to derive the conditional distribution function $P_{Y_k^n|X_k^n}(\boldsymbol{y}_k^n|\boldsymbol{x}_k^n)$ as follows:

$$P_{Y_k^n|X_k^n}(\boldsymbol{y}_k^n|\boldsymbol{x}_k^n) = \frac{1}{\left[2\pi\left(N_{I_k^{(l)}}(\boldsymbol{r}) + N_k(r_k)\right)\right]^{\frac{n}{2}}} \times \exp\left\{-\frac{\left\|\boldsymbol{y}_k^n - \mathbb{E}\left[I_k^{(l)}(\boldsymbol{r})\right]\mathbf{I}_n - \boldsymbol{x}_k^n\right\|^2}{2\left[N_{I_k^{(l)}}(\boldsymbol{r}) + N_k(r_k)\right]}\right\} \tag{55}$$

where $\|\cdot\|$ is the Euclidean norm and $\mathbf{I}_n$ is the identity matrix with size n.

Step 2: To derive the modified information density $\boldsymbol{i}(\boldsymbol{x}_k^n; \boldsymbol{y}_k^n)$, we need to apply the mean and variance of interference derived in Eqs. (23) and (25) and select the reference output distribution for the THz wireless channel as $Q_{Y_k^n}(\boldsymbol{y}_k^n) = \mathcal{N}\left(\mathbb{E}\left[I_k^{(l)}(\boldsymbol{r})\right]\mathbf{I}_n, \left(\mathcal{P}_k\mathcal{P}_{\text{total}}(r_k) + N_{I_k^{(l)}}(\boldsymbol{r}) + N_k(r_k)\right)\mathbf{I}_n\right)$.

Step 3: Using Eqs. (53) and (55), we derive the *modified information density* $\boldsymbol{i}(\boldsymbol{x}_k^n; \boldsymbol{y}_k^n)$ as follows:

$$\begin{aligned}
\boldsymbol{i}(\boldsymbol{x}_k^n; \boldsymbol{y}_k^n) &= \frac{1}{n}\log_2\left\{\frac{\left[2\pi\left(\mathcal{P}_k\mathcal{P}_{\text{total}}(r_k) + N_{I_k^{(l)}}(\boldsymbol{r}) + N_k(r_k)\right)\right]^{\frac{n}{2}}}{\left[2\pi\left(N_{I_k^{(l)}}(\boldsymbol{r}) + N_k(r_k)\right)\right]^{\frac{n}{2}}} \times \exp\left\{-\frac{\left\|\boldsymbol{y}_k^n - \mathbb{E}\left[I_k^{(l)}(\boldsymbol{r})\right]\mathbf{I}_n - \boldsymbol{x}_k^n\right\|^2}{2\left[N_{I_k^{(l)}}(\boldsymbol{r}) + N_k(r_k)\right]}\right\} \times \exp\left\{\frac{\left\|\boldsymbol{y}_k^n - \mathbb{E}\left[I_k^{(l)}(\boldsymbol{r})\right]\mathbf{I}_n\right\|^2}{2\left[\mathcal{P}_k\mathcal{P}_{\text{total}}(r_k) + N_{I_k^{(l)}}(\boldsymbol{r}) + N_k(r_k)\right]}\right\}\right\} \\
&= \frac{1}{n}\log_2\left\{\frac{\left[2\pi\left(\mathcal{P}_k\mathcal{P}_{\text{total}}(r_k) + N_{I_k^{(l)}}(\boldsymbol{r}) + N_k(r_k)\right)\right]^{\frac{n}{2}}}{\left[2\pi\left(N_{I_k^{(l)}}(\boldsymbol{r}) + N_k(r_k)\right)\right]^{\frac{n}{2}}}\right\} + \frac{(\log_2 e)}{2n}\left[\frac{\left\|\boldsymbol{y}_k^n - \mathbb{E}\left[I_k^{(l)}(\boldsymbol{r})\right]\mathbf{I}_n\right\|^2}{\mathcal{P}_k\mathcal{P}_{\text{total}}(r_k) + N_{I_k^{(l)}}(\boldsymbol{r}) + N_k(r_k)} - \frac{\left\|\boldsymbol{y}_k^n - \mathbb{E}\left[I_k^{(l)}(\boldsymbol{r})\right]\mathbf{I}_n - \boldsymbol{x}_k^n\right\|^2}{N_{I_k^{(l)}}(\boldsymbol{r}) + N_k(r_k)}\right] \\
&= \frac{1}{2}\log_2\left[\frac{\mathcal{P}_k\mathcal{P}_{\text{total}}(r_k) + N_{I_k^{(l)}}(\boldsymbol{r}) + N_k(r_k)}{N_{I_k^{(l)}}(\boldsymbol{r}) + N_k(r_k)}\right] + \frac{(\log_2 e)}{2n}\left[\frac{\left\|\boldsymbol{y}_k^n - \mathbb{E}\left[I_k^{(l)}(\boldsymbol{r})\right]\mathbf{I}_n\right\|^2}{\mathcal{P}_k\mathcal{P}_{\text{total}}(r_k) + N_{I_k^{(l)}}(\boldsymbol{r}) + N_k(r_k)} - \frac{\left\|\boldsymbol{y}_k^n - \mathbb{E}\left[I_k^{(l)}(\boldsymbol{r})\right]\mathbf{I}_n - \boldsymbol{x}_k^n\right\|^2}{N_{I_k^{(l)}}(\boldsymbol{r}) + N_k(r_k)}\right].
\end{aligned} \tag{56}$$

Using Eq. (12), we obtain the following equation:

$$\begin{aligned}
\boldsymbol{i}(\boldsymbol{x}_k^n; \boldsymbol{y}_k^n) &= \frac{1}{2}\log_2\left[\frac{\mathcal{P}_k\mathcal{P}_{\text{total}}(r_k) + N_{I_k^{(l)}}(\boldsymbol{r}) + N_k(r_k)}{N_{I_k^{(l)}}(\boldsymbol{r}) + N_k(r_k)}\right] + \frac{(\log_2 e)}{2n}\left[\left\|\sqrt{\mathcal{P}_{\text{total}}(r_k)}\boldsymbol{x}_k^n + \sum_{i=1, i\neq k}^{K+1}\sqrt{\mathcal{P}_{\text{total}}(r_i)}\boldsymbol{x}_i^n + \boldsymbol{n}_k - \mathbb{E}\left[I_k^{(l)}(\boldsymbol{r})\right]\mathbf{I}_n\right\|^2\left\{\mathcal{P}_k\mathcal{P}_{\text{total}}(r_k) + N_{I_k^{(l)}}(\boldsymbol{r}) + N_k(r_k)\right\}^{-1}\right. \\
&\quad \left. - \left\|\sqrt{\mathcal{P}_{\text{total}}(r_k)}\boldsymbol{x}_k^n + \sum_{i=1, i\neq k}^{K+1}\sqrt{\mathcal{P}_{\text{total}}(r_i)}\boldsymbol{x}_i^n + \boldsymbol{n}_k\right.\right.
\end{aligned}$$

$$-\mathbb{E}\left[I_k^{(l)}(\boldsymbol{r})\right]\mathbf{I}_n-\boldsymbol{x}_k^n\Big\|^2\left\{N_{I_k^{(l)}}(\boldsymbol{r})+N_k(r_k)\right\}^{-1}\Bigg]. \quad (57)$$

Step 4: Using Eqs. (53) and (57), we can derive an *upper-bound* on the mutual information $I(\boldsymbol{x}_k^n,\boldsymbol{y}_k^n)$ as follows:

$$\begin{aligned}
I(\boldsymbol{x}_k^n,\boldsymbol{y}_k^n) &= \mathbb{E}\left[\frac{1}{2}\log_2\left[\frac{\mathcal{P}_k\mathcal{P}_{\text{total}}(r_k)+N_{I_k^{(l)}}(\boldsymbol{r})+N_k(r_k)}{N_{I_k^{(l)}}(\boldsymbol{r})+N_k(r_k)}\right]\right.\\
&+\frac{(\log_2 e)}{2n}\left\{\left\|\sqrt{\mathcal{P}_{\text{total}}(r_k)}\boldsymbol{x}_k^n+\sum_{i=1,i\neq k}^{K+1}\sqrt{\mathcal{P}_{\text{total}}(r_i)}\boldsymbol{x}_i^n+\boldsymbol{n}_k\right.\right.\\
&-\mathbb{E}\left[I_k^{(l)}(\boldsymbol{r})\right]\mathbf{I}_n\Big\|^2\left\{\mathcal{P}_k\mathcal{P}_{\text{total}}(r_k)+N_{I_k^{(l)}}(\boldsymbol{r})+N_k(r_k)\right\}^{-1}\\
&-\left\|\sqrt{\mathcal{P}_{\text{total}}(r_k)}\boldsymbol{x}_k^n+\sum_{i=1,i\neq k}^{K+1}\sqrt{\mathcal{P}_{\text{total}}(r_i)}\boldsymbol{x}_i^n+\boldsymbol{n}_k\right.\\
&\left.\left.\left.-\mathbb{E}\left[I_k^{(l)}(\boldsymbol{r})\right]\mathbf{I}_n-\boldsymbol{x}_k^n\right\|^2\left\{N_{I_k^{(l)}}(\boldsymbol{r})+N_k(r_k)\right\}^{-1}\right\}\right]\\
&\leq\frac{1}{2}\log_2\left[\frac{\mathcal{P}_k\mathcal{P}_{\text{total}}(r_k)+N_{I_k^{(l)}}(\boldsymbol{r})+N_k(r_k)}{N_{I_k^{(l)}}(\boldsymbol{r})+N_k(r_k)}\right]+\frac{(\log_2 e)}{n}\\
&\times\left\{\mathbb{E}\left[\left\|\sqrt{\mathcal{P}_{\text{total}}(r_k)}\boldsymbol{x}_k^n\right\|^2+\left\|\sum_{i=1,i\neq k}^{K+1}\sqrt{\mathcal{P}_{\text{total}}(r_i)}\boldsymbol{x}_i^n-\mathbb{E}\left[I_k^{(l)}(\boldsymbol{r})\right]\right.\right.\right.\\
&\left.\left.\left.\times\mathbf{I}_n\right\|^2+\|\boldsymbol{n}_k\|^2\right]\left\{\mathcal{P}_k\mathcal{P}_{\text{total}}(r_k)+N_{I_k^{(l)}}(\boldsymbol{r})+N_k(r_k)\right\}^{-1}\right.\\
&-\mathbb{E}\left[\left\|\sqrt{\mathcal{P}_{\text{total}}(r_k)}\boldsymbol{x}_k^n\right\|^2+\left\|\sum_{i=1,i\neq k}^{K+1}\sqrt{\mathcal{P}_{\text{total}}(r_i)}\boldsymbol{x}_i^n\right.\right.\\
&\left.\left.\left.-\mathbb{E}\left[I_k^{(l)}(\boldsymbol{r})\right]\mathbf{I}_n\right\|^2+\|\boldsymbol{n}_k\|^2+\|\boldsymbol{x}_k^n\|^2\right]\left\{N_{I_k^{(l)}}(\boldsymbol{r})+N_k(r_k)\right\}^{-1}\right\}\\
&=\frac{1}{2}\log_2\left[\frac{\mathcal{P}_k\mathcal{P}_{\text{total}}(r_k)+N_{I_k^{(l)}}(\boldsymbol{r})+N_k(r_k)}{N_{I_k^{(l)}}(\boldsymbol{r})+N_k(r_k)}\right]\\
&-(\log_2 e)\left[\frac{\mathcal{P}_k\left[\mathcal{P}_{\text{total}}(r_k)+1\right]}{N_{I_k^{(l)}}(\boldsymbol{r})+N_k(r_k)}\right] \quad (58)
\end{aligned}$$

which is Eq. (54), completing the proof for Theorem 2. ■

Remarks on Theorem 2: While it is infeasible to derive the exact closed-form expression for the channel capacity $C(r_k,\mathcal{P}_k)$ in terms of the mutual information for our proposed statistical delay and error-rate bounded QoS provisioning in supporting mURLLC over FBC-EH based 6G THz wireless nano-networks in the finite blocklength regime, Theorem 2 yields the accurate upper-bound for the mutual information $I(\boldsymbol{x}_k^n,\boldsymbol{y}_k^n)$ derived in Eq. (54) is an accurate approximation for the channel capacity $C(r_k,\mathcal{P}_k)$ given by Eq. (52), which provides with practically very useful designing guidance for engineering, modeling, and evaluating our proposed statistical delay and error-rate bounded QoS provisioning in supporting mURLLC over FBC-EH based 6G THz wireless nano-networks in the finite blocklength regime.

D. The Channel Dispersion Modeling for the THz Band Communications in the Finite Blocklength Regime

Generally speaking, it is challenging to derive the closed-form expression of the channel dispersion for the nano-communications schemes in the THz band using FBC. However, leveraging some mathematical manipulations, we can obtain the tight upper-bound for the channel dispersion $V(r_k,\mathcal{P}_k)$ for our proposed statistical delay and error-rate bounded QoS provisioning schemes in supporting mURLLC over FBC-EH based 6G THz wireless nano-networks as summarized in the following theorem.

Theorem 3: The upper-bound on the *channel dispersion* $V(r_k,\mathcal{P}_k)$ for our proposed statistical delay and error-rate bounded QoS provisioning in supporting mURLLC over FBC-EH based 6G THz wireless nano-networks is given as follows:

$$V(r_k,\mathcal{P}_k)\leq 8n(\log_2 e)^2\left[\mathcal{P}_k+N_{I_k^{(l)}}(\boldsymbol{r})+N_k(r_k)\right]. \quad (59)$$

Proof: To derive the upper-bound on the channel dispersion $V(r_k,\mathcal{P}_k)$, we need to proceed with the following two steps.

Step 1: We start with variance of the modified information density $\boldsymbol{i}(\boldsymbol{x}_k^n;\boldsymbol{y}_k^n)$ as in the following equation:

$$\begin{aligned}
V(r_k,\mathcal{P}_k)&=\text{Var}\left[\boldsymbol{i}(\boldsymbol{x}_k^n;\boldsymbol{y}_k^n)\right]=\frac{1}{n}\text{Var}\left[\log_2\left(\frac{P_{Y_k^n|X_k^n}(\boldsymbol{y}_k^n|\boldsymbol{x}_k^n)}{Q_{Y_k^n}(\boldsymbol{y}_k^n)}\right)\right]\\
&\leq\frac{2}{n}\left\{\text{Var}\left[\log_2\left(P_{Y_k^n|X_k^n}(\boldsymbol{y}_k^n|\boldsymbol{x}_k^n)\right)\right]+\text{Var}\left[\log_2\left(Q_{Y_k^n}(\boldsymbol{y}_k^n)\right)\right]\right\}
\end{aligned} \quad (60)$$

where $\text{Var}[\cdot]$ represents the variance operation.

Step 2: We can apply the Poincará inequality to derive the following equation:

$$\begin{aligned}
&\text{Var}\left[\log_2\left(P_{Y_k^n|X_k^n}(\boldsymbol{y}_k^n|\boldsymbol{x}_k^n)\right)\right]\\
&\leq\mathbb{E}\left[\left\|\nabla\log_2\left(P_{Y_k^n|X_k^n}(\boldsymbol{y}_k^n|\boldsymbol{x}_k^n)\right)\right\|^2\right]
\end{aligned} \quad (61)$$

where ∇ is the Nabla operator. Then, to calculate the function $\nabla\log_2\left(P_{Y_k^n|X_k^n}(\boldsymbol{y}_k^n|\boldsymbol{x}_k^n)\right)$, we have

$$\begin{aligned}
&\nabla\log_2\left(P_{Y_k^n|X_k^n}(\boldsymbol{y}_k^n|\boldsymbol{x}_k^n)\right)\\
&=\frac{(\log_2 e)}{P_{Y_k^n|X_k^n}(\boldsymbol{y}_k^n|\boldsymbol{x}_k^n)}\nabla P_{Y_k^n|X_k^n}(\boldsymbol{y}_k^n|\boldsymbol{x}_k^n)\\
&=\frac{(\log_2 e)}{P_{Y_k^n|X_k^n}(\boldsymbol{y}_k^n|\boldsymbol{x}_k^n)}\sum_{m=1}^{M}\left\{\frac{1}{M}\left[2\pi\left(N_{I_k^{(l)}}(\boldsymbol{r})+N_k(r_k)\right)\right]^{-\frac{n}{2}}\right.\\
&\left.\times\nabla\exp\left\{-\frac{\|\boldsymbol{y}_k^n-\mathbb{E}\left[I_k^{(l)}(\boldsymbol{r})\right]\mathbf{I}_n-\boldsymbol{x}_k^n(m)\|^2}{2\left[N_{I_k^{(l)}}(\boldsymbol{r})+N_k(r_k)\right]}\right\}\right\}\\
&=\frac{(\log_2 e)}{P_{Y_k^n|X_k^n}(\boldsymbol{y}_k^n|\boldsymbol{x}_k^n)}\sum_{m=1}^{M}\left\{\frac{1}{M}\left[2\pi\left(N_{I_k^{(l)}}(\boldsymbol{r})+N_k(r_k)\right)\right]^{-\frac{n}{2}}\right.\\
&\left.\times\left(\boldsymbol{x}_k^n(m)+\mathbb{E}\left[I_k^{(l)}(\boldsymbol{r})\right]\mathbf{I}_n-\boldsymbol{y}_k^n\right)\right.
\end{aligned}$$

$$\times \exp\left\{-\frac{\left\|\boldsymbol{y}_k^n - \mathbb{E}\left[I_k^{(l)}(\boldsymbol{r})\right]\mathbf{I}_n - \boldsymbol{x}_k^n(m)\right\|^2}{2\left[N_{I_k^{(l)}}(\boldsymbol{r}) + N_k(r_k)\right]}\right\}\Bigg\}$$
$$= (\log_2 e)\left\{\mathbb{E}\left[\boldsymbol{x}_k^n|\boldsymbol{y}_k^n\right] + \mathbb{E}\left[I_k^{(l)}(\boldsymbol{r})\right]\mathbf{I}_n - \boldsymbol{y}_k^n\right\} \quad (62)$$

where $\boldsymbol{x}_k^n(m)$ is the encoded signal from message $m \in \mathcal{M}$ with length n at nano transmitter k. Let us define:

$$\widehat{\boldsymbol{x}}_k^n \triangleq \mathbb{E}\left[\boldsymbol{x}_k^n|\boldsymbol{y}_k^n\right]. \quad (63)$$

Accordingly, using the average power constraint given in Eq. (11), we can obtain the following equation:

$$\begin{aligned}
&\mathrm{Var}\left[\log_2\left(P_{Y_k^n|X_k^n}\left(\boldsymbol{y}_k^n|\boldsymbol{x}_k^n\right)\right)\right] \\
&\le (\log_2 e)^2\mathbb{E}\left[\left\|\widehat{\boldsymbol{x}}_k^n + \mathbb{E}\left[I_k^{(l)}(\boldsymbol{r})\right]\mathbf{I}_n - \boldsymbol{y}_k^n\right\|^2\right] \\
&\le 2(\log_2 e)^2\left\{\mathbb{E}\left[\|\widehat{\boldsymbol{x}}_k^n\|^2\right] + \mathbb{E}\left[\left\|\boldsymbol{y}_k^n - \mathbb{E}\left[I_k^{(l)}(\boldsymbol{r})\right]\right\|^2\right]\right\} \\
&= 2(\log_2 e)^2\left\{n\mathcal{P}_k + n\left[N_{I_k^{(l)}}(\boldsymbol{r}) + N_k(r_k)\right]\right\} \\
&= 2n(\log_2 e)^2\left[\mathcal{P}_k + N_{I_k^{(l)}}(\boldsymbol{r}) + N_k(r_k)\right]. \quad (64)
\end{aligned}$$

Similarly, we can derive the function $\mathrm{Var}\left[\log_2\left(Q_{Y_k^n}\left(\boldsymbol{y}_k^n\right)\right)\right]$ as follows:

$$\mathrm{Var}\left[\log_2\left(Q_{Y_k^n}\left(\boldsymbol{y}_k^n\right)\right)\right] \le 2n(\log_2 e)^2\left[\mathcal{P}_k + N_{I_k^{(l)}}(\boldsymbol{r}) + N_k(r_k)\right]. \quad (65)$$

Therefore, plugging Eqs. (64) and (65) back into Eq. (60), we get:

$$V(r_k, \mathcal{P}_k) \le 8n(\log_2 e)^2\left[\mathcal{P}_k + N_{I_k^{(l)}}(\boldsymbol{r}) + N_k(r_k)\right] \quad (66)$$

which is Eq. (59), completing the proof for Theorem 3. ■

Remarks on Theorem 3: The upper-bound on the channel dispersion $V(r_k, \mathcal{P}_k)$ given in Eq. (59) proved in Theorem 3 is important to derive the maximum achievable coding rate $R(n, r_k, \mathcal{P}_k)$ specified by Eq. (19), and thereafter, the ϵ-effective capacity $EC_\epsilon(\theta_k)$ defined by Eq. (51), and finally, solve the joint optimization problem for resource allocations to support our proposed statistical delay and error-rate bounded QoS provisioning for mURLLC over FBC-EH 6G THz wireless nano-networks which are to be investigated in Section IV-B.

IV. Joint Optimal Resource Allocation for Our Proposed Statistical Delay and Error-Rate Bounded QoS Provisioning for mURLLC Over FBC-EH 6G THz Wireless Nano-Networks

In this section, we derive the optimal resource allocation policies for our proposed statistical delay and error-rate bounded QoS provisioning in supporting mURLLC over FBC-EH based 6G THz wireless nano-networks.

A. The Set of EH Constraints in the THz Band

1) Transmit Power Constraint: Due to the limitation of the energy harvested at the nanogenerator, we can derive the minimum required energy, denoted by $\mathcal{P}_{\min}$, for transmitting one data packet at each self-powered nano device as follows:

$$\mathcal{P}_{\min} = \zeta_k\mathcal{P}_k + \mathcal{P}_{\text{circuit}} \quad (67)$$

where ζ_k is the reciprocal of drain efficiency of power amplifier and $\mathcal{P}_{\text{circuit}}$ consists of two components, i.e., power consumption of the transmitter circuit and the receiver circuit, which is independent of the transmission distance. Then, we can derive the relationship between harvested energy after n_{cyc} cycles and the minimum required energy for transmitting a data packet with length n as follows:

$$\frac{1}{2}C_{\text{cap}}\left[V_{\text{cap}}(n_{\text{cyc}})\right]^2 \ge n\left(\zeta_k\mathcal{P}_k + \mathcal{P}_{\text{circuit}}\right). \quad (68)$$

Plugging Eq. (14) into Eq. (68), we have

$$\frac{1}{2}C_{\text{cap}}\left\{V_g\left[1 - \exp\left(-\frac{n_{\text{cyc}}\Delta Q}{V_g C_{\text{cap}}}\right)\right]\right\}^2 \ge n\left(\zeta_k\mathcal{P}_k + \mathcal{P}_{\text{circuit}}\right). \quad (69)$$

Accordingly, we can derive a lower bound on the number of cycles n_{cyc} for self-powered nano devices as in the following inequation:

$$n_{\text{cyc}} \ge -\frac{C_{\text{cap}}V_g}{\Delta Q}\log\left[1 - \sqrt{\frac{2n}{C_{\text{cap}}V_g}\left(\zeta_k\mathcal{P}_k + \mathcal{P}_{\text{circuit}}\right)}\right]. \quad (70)$$

According to Eq. (70), to guarantee the effective value of a lower bound on n_{cyc}, we have

$$\sqrt{\frac{2n}{C_{\text{cap}}V_g}\left(\zeta_k\mathcal{P}_k + \mathcal{P}_{\text{circuit}}\right)} \le 1. \quad (71)$$

Correspondingly, we can derive an upper-bound on the transmit power $\mathcal{P}_k$ for the self-powered nano transmitter k as follows:

$$\mathcal{P}_k \le \frac{C_{\text{cap}}V_g}{2n\zeta_k} - \frac{P_{\text{circuit}}}{\zeta_k}. \quad (72)$$

2) Energy Harvesting Rate Constraint: To derive the EH rate constraint, first we need to calculate the energy consumption rate, denoted by λ_{ec}, of each self-powered nano device as follows:

$$\lambda_{\text{ec}} < \mathcal{P}_k nC(r_k, \mathcal{P}_k). \quad (73)$$

As a result, the energy consumption rate λ_{ec} should not be greater than the energy harvesting rate λ_{eh} given in Eq. (16), i.e., $\lambda_{\text{ec}} \le \lambda_{\text{eh}}$. Then, using Eq. (16) and (73), we can derive an upper-bound on the transmit power $\mathcal{P}_k$ for our proposed statistical delay and error-rate bounded QoS provisioning in supporting mURLLC over FBC-EH based 6G THz wireless nano-networks as follows:

$$\mathcal{P}_k \le \frac{V_g\Delta Q}{nC(r_k, \mathcal{P}_k)t_{\text{cyc}}}\left[\exp\left(-\frac{\Delta Q n_{\text{cyc}}}{V_g C_{\text{cap}}}\right) - \exp\left(-\frac{2\Delta Q n_{\text{cyc}}}{V_g C_{\text{cap}}}\right)\right]. \quad (74)$$

B. Joint Optimal Resource Allocation for Our Proposed Statistical Delay and Error-Rate Bounded QoS Provisioning for mURLLC Over FBC-EH 6G THz Wireless Nano-Networks

The function of ϵ-effective capacity $EC_{\epsilon}(\theta_k)$ depends on the transmit power $\mathcal{P}_k$ and blocklength n. To maximize the ϵ-effective capacity $EC_{\epsilon}(\theta_k)$ while guaranteeing the EH constraints among self-powered nano devices for our proposed statistical delay and error-rate bounded QoS provisioning in supporting mURLLC over FBC-EH based 6G THz wireless nano-networks, we can formulate the optimization problem $\mathbf{P_1}$ subject to the EH constraints given by Eqs. (72) and (74) as follows:

$$\mathbf{P_1}: \arg \max_{\{n, \mathcal{P}_k\}} EC_{\epsilon}(\theta_k) \tag{75}$$

$$\text{s.t.: } \mathbf{C1:} R(n, r_k, \mathcal{P}_k) \approx C(r_k, \mathcal{P}_k) - \sqrt{\frac{V(r_k, \mathcal{P}_k)}{n}} Q^{-1}(\epsilon_k); \tag{76}$$

$$\mathbf{C2:} \mathcal{P}_k \leq \min \Bigg\{ \frac{C_{\text{cap}} V_g}{2n\zeta_k} - \frac{P_{\text{circuit}}}{\zeta_k}, \frac{V_g \Delta Q}{nC(r_k, \mathcal{P}_k) t_{\text{cyc}}} \times \left[\exp\left(-\frac{\Delta Q n_{\text{cyc}}}{V_g C_{\text{cap}}} \right) - \exp\left(-\frac{2\Delta Q n_{\text{cyc}}}{V_g C_{\text{cap}}} \right) \right] \Bigg\}; \tag{77}$$

$$\mathbf{C3:} \mathcal{P}_k \geq \frac{1}{(r_k)^{-\eta} G 10^{\frac{\xi_k}{10}} S(f)} \left[\frac{\gamma_{\text{th}} \left(N_k(r_k) + N_{I_k^{(l)}}(\boldsymbol{r}) \right)}{\left(\frac{c}{4\pi f r_k} \right) e^{-\frac{\alpha_{\text{abs}} r_k}{2}}} \right]^2; \tag{78}$$

$$\mathbf{C4:} \mathcal{P}_k > 0. \tag{79}$$

Equivalently, we can derive a minimization problem $\mathbf{P_2}$ as follows:

$$\mathbf{P_2}: \arg \min_{\{n, \mathcal{P}_k\}} \mathbb{E}_{r_k} \Bigg\{ \epsilon_k + (1 - \epsilon_k) \exp \Bigg\{ -\theta_k n \Bigg[C(r_k, \mathcal{P}_k) - \sqrt{\frac{V(r_k, \mathcal{P}_k)}{n}} Q^{-1}(\epsilon_k) \Bigg] \Bigg\} \Bigg\} \tag{80}$$

subject to the same constraints given in **C2**, **C3**, and **C4** which are specified by Eqs. (77), (78), and (79), respectively, in optimization problem $\mathbf{P_1}$. In order to solve the minimization problem $\mathbf{P_2}$, we define an utility function $F(n, r_k, \mathcal{P}_k)$ as follows:

$$F(n, r_k, \mathcal{P}_k) \triangleq nR(n, r_k, \mathcal{P}_k). \tag{81}$$

Then, by plugging Eq. (81) back into Eq. (80), we can rewrite the ϵ-effective capacity as follows:

$$EC_{\epsilon}(\theta_k) \triangleq -\frac{1}{\theta_k} \log \left(\mathbb{E}_{r_k} \left[\epsilon_k + (1 - \epsilon_k) e^{-\theta_k F(n, r_k, \mathcal{P}_k)} \right] \right). \tag{82}$$

We can formulate a new maximization problem $\mathbf{P_3}$, which is equivalent to $\mathbf{P_2}$, for our proposed statistical delay and error-rate bounded QoS provisioning in supporting mURLLC over FBC-EH based 6G THz wireless nano-networks as follows:

$$\mathbf{P_3}: \arg \max_{\{n, \mathcal{P}_k\}} F(n, r_k, \mathcal{P}_k) \tag{83}$$

subject to the same constraints given in **C2**, **C3**, and **C4** which are specified by Eqs. (77), (78), and (79), respectively, in optimization problem $\mathbf{P_1}$. To analyze the monotonicity of problem $\mathbf{P_3}$, we investigate the first-order derivative of the function $F(n, r_k, \mathcal{P}_k)$ with respect to the blocklength n when $\epsilon_k \in (0, 0.5)$ as follows:

$$\begin{aligned} \frac{\partial F(n, r_k, \mathcal{P}_k)}{\partial n} &= \frac{\partial nC(r_k, \mathcal{P}_k)}{\partial n} - \frac{\partial \left[\sqrt{nV(r_k, \mathcal{P}_k)} Q^{-1}(\epsilon_k) \right]}{\partial n} \\ &= C(r_k, \mathcal{P}_k) - \frac{\sqrt{V(r_k, \mathcal{P}_k)} Q^{-1}(\epsilon_k)}{2\sqrt{n}} \\ &= R(n, r_k, \mathcal{P}_k) + \frac{\sqrt{V(r_k, \mathcal{P}_k)} Q^{-1}(\epsilon_k)}{2\sqrt{n}} > 0. \end{aligned} \tag{84}$$

As a result, the optimization problem $\mathbf{P_3}$ specified by Eq. (83) is a monotonically increasing function of blocklength n when the error probability $\epsilon_k \in (0, 0.5)$. Then, the theorem that follows bellow characterizes the concavity of the optimization problem $\mathbf{P_3}$ with respect to the transmit power $\mathcal{P}_k$.

Theorem 4: Let the error probability be $\epsilon_k \in (0, 0.5)$ for our proposed statistical delay and error-rate bounded QoS provisioning in supporting mURLLC over FBC-EH based 6G THz wireless nano-networks and define the minimum blocklength, denoted by $n_{\min}$, as the function of ϵ_k, $\mathcal{P}_k$, $\mathcal{P}_{\text{total}}(r_k)$, $N_{I_k^{(l)}}(\boldsymbol{r})$, and $N_k(r_k)$ as follows:

$$n_{\min} \triangleq \frac{2 \left[Q^{-1}(\epsilon_k) \right]^2 \left[\mathcal{P}_k + N_{I_k^{(l)}}(\boldsymbol{r}) + N_k(r_k) \right]}{\left[\mathcal{P}_{\text{total}}(r_k) \right]^4}. \tag{85}$$

If the blocklength n satisfies following condition for $n_{\min}$ given by Eq. (85):

$$n > n_{\min}, \tag{86}$$

then the optimization problem $\mathbf{P_3}$ specified by Eq. (83) is *strictly concave* with respect to the transmit power $\mathcal{P}_k$.

Proof: To prove this theorem, we need to proceed with the following two steps.

Step 1: We take the first-order derivative over the utility function $F(n, r_k, \mathcal{P}_k)$ specified in Eq. (81) with respect to the transmit power $\mathcal{P}_k$ as follows:

$$\begin{aligned} \frac{\partial F(n, r_k, \mathcal{P}_k)}{\partial \mathcal{P}_k} &= \frac{\partial \left[nC(r_k, \mathcal{P}_k) - \sqrt{nV(r_k, \mathcal{P}_k)} Q^{-1}(\epsilon_k) \right]}{\partial \mathcal{P}_k} \\ &= \frac{\partial nC(r_k, \mathcal{P}_k)}{\partial \mathcal{P}_k} - \frac{\partial \left[\sqrt{nV(r_k, \mathcal{P}_k)} Q^{-1}(\epsilon_k) \right]}{\partial \mathcal{P}_k} \\ &= \frac{n \mathcal{P}_{\text{total}}(r_k)}{2(\log 2) \left[\mathcal{P}_k \mathcal{P}_{\text{total}}(r_k) + N_{I_k^{(l)}}(\boldsymbol{r}) + N_k(r_k) \right]} \\ &\quad - n(\log_2 e) \left[\frac{\mathcal{P}_{\text{total}}(r_k) + 1}{N_{I_k^{(l)}}(\boldsymbol{r}) + N_k(r_k)} \right] \\ &\quad - \frac{\sqrt{2n} (\log_2 e) Q^{-1}(\epsilon_k)}{\sqrt{\mathcal{P}_k + N_{I_k^{(l)}}(\boldsymbol{r}) + N_k(r_k)}}. \end{aligned} \tag{87}$$

Step 2: We take the second-order derivative of the function $F(n, r_k, \mathcal{P}_k)$ with respect to the transmit power $\mathcal{P}_k$ as follows:

$$\frac{\partial^2 F(n,r_k,\mathcal{P}_k)}{\partial \mathcal{P}_k^2} = \frac{\sqrt{2n}(\log_2 e)Q^{-1}(\epsilon_k)}{2\left[\mathcal{P}_k + N_{I_k^{(l)}}(\boldsymbol{r}) + N_k(r_k)\right]^{\frac{3}{2}}} - \frac{n\left[\mathcal{P}_{\text{total}}(r_k)\right]^2}{2(\log 2)\left[\mathcal{P}_k\mathcal{P}_{\text{total}}(r_k) + N_{I_k^{(l)}}(\boldsymbol{r}) + N_k(r_k)\right]^2}. \tag{88}$$

Applying the fact of $\mathcal{P}_{\text{total}}(r_k) < 1$ into Eq. (88), we get:

$$\begin{aligned}\frac{\partial^2 F(n,r_k,\mathcal{P}_k)}{\partial \mathcal{P}_k^2} &= \frac{\sqrt{2n}(\log_2 e)Q^{-1}(\epsilon_k)}{2\left[\mathcal{P}_k + N_{I_k^{(l)}}(\boldsymbol{r}) + N_k(r_k)\right]^{\frac{3}{2}}} - \frac{n\left[\mathcal{P}_{\text{total}}(r_k)\right]^2}{2(\log 2)\left[\mathcal{P}_k\mathcal{P}_{\text{total}}(r_k) + N_{I_k^{(l)}}(\boldsymbol{r}) + N_k(r_k)\right]^2} \\ &\leq \frac{\sqrt{2n}(\log_2 e)Q^{-1}(\epsilon_k)}{2\left[\mathcal{P}_k + N_{I_k^{(l)}}(\boldsymbol{r}) + N_k(r_k)\right]^{\frac{3}{2}}} - \frac{n\left[\mathcal{P}_{\text{total}}(r_k)\right]^2}{2(\log 2)\left[\mathcal{P}_k + N_{I_k^{(l)}}(\boldsymbol{r}) + N_k(r_k)\right]^2} \\ &= \frac{\sqrt{2n}Q^{-1}(\epsilon_k)\sqrt{\mathcal{P}_k + N_{I_k^{(l)}}(\boldsymbol{r}) + N_k(r_k)} - n\left[\mathcal{P}_{\text{total}}(r_k)\right]^2}{2(\log 2)\left[\mathcal{P}_k + N_{I_k^{(l)}}(\boldsymbol{r}) + N_k(r_k)\right]^2} \\ &= \frac{\left(\sqrt{nn_{\min}} - n\right)\left[\mathcal{P}_{\text{total}}(r_k)\right]^2}{2(\log 2)\left[\mathcal{P}_k + N_{I_k^{(l)}}(\boldsymbol{r}) + N_k(r_k)\right]^2}\end{aligned} \tag{89}$$

where $n_{\min}$ is given by Eq. (85). Applying the condition: $n > n_{\min}$ specified by Eq. (86) into Eq. (89), which implies that $(\sqrt{nn_{\min}} - n) < 0$, and thus we can obtain the following equation:

$$\frac{\partial^2 F(n,r_k,\mathcal{P}_k)}{\partial \mathcal{P}_k^2} < 0. \tag{90}$$

Therefore, we complete the proof for Theorem 4. ■

Remarks on Theorem 4: Theorem 4 implies that if the finite blocklength is lower-bounded by the minimum blocklength $n_{\min}$ given by Eq. (85), then there exists the unique optimal power allocation policy that maximizes the ϵ-effective capacity in the THz band in the finite blocklength regime. Note that $n_{\min}$ is proportional to noise and interference power, and the decoding error probability ϵ_k but inversely proportional to the total received power $\mathcal{P}_{\text{total}}(r_k)$. These observations are expected because the more noisy and interfered channels warrant the longer coding blocklength for the more powerful channel-coding error-control performance. Then, the theorem that follows bellow derives the closed-form expressions of the optimal transmit power for our proposed schemes.

Theorem 5: **If** the blocklength $n > n_{\min}$, which is given by Eq. (85), for our proposed statistical delay and error-rate bounded QoS provisioning in supporting mURLLC over FBC-EH based 6G THz wireless nano-networks, **then** depending on whether the SINR falls into the high-range, medium-range, and low-range regions, the optimal transmit power policies are given by the following three claims, respectively:

Claim 1: **If** the SINR falls into a high-range region, which is defined as follows:

$$\mathcal{P}_k\mathcal{P}_{\text{total}}(r_k) \gg N_{I_k^{(l)}}(\boldsymbol{r}) + N_k(r_k), \tag{91}$$

then the optimal power allocation policy for the high-range SINR region, denoted by $\mathcal{P}_k^{\text{OPT,H}}$, at nano transmitter k is given as follows:

$$\mathcal{P}_k^{\text{OPT,H}} = \frac{n}{2}\left\{Q^{-1}(\epsilon_k) + \left\{\left[Q^{-1}(\epsilon_k)\right]^2 + (\log 2)(\lambda_1 - \lambda_2) + n\left[\frac{\mathcal{P}_{\text{total}}(r_k)+1}{N_{I_k^{(l)}}(\boldsymbol{r}) + N_k(r_k)}\right]\right\}^{\frac{1}{2}}\right\}^{-2}. \tag{92}$$

Claim 2: **If** the SINR falls into a low-range region, which is defined as follows:

$$\mathcal{P}_k\mathcal{P}_{\text{total}}(r_k) \ll N_{I_k^{(l)}}(\boldsymbol{r}) + N_k(r_k), \tag{93}$$

then the optimal power allocation policy for the low-range SINR region, denoted by $\mathcal{P}_k^{\text{OPT,L}}$, at nano transmitter k is given as follows:

$$\mathcal{P}_k^{\text{OPT,L}} = \frac{2nQ^{-1}(\epsilon_k)}{\left\{(\log 2)(\lambda_2 - \lambda_1) - \frac{2n + n\mathcal{P}_{\text{total}}(r_k)}{2\left[N_{I_k^{(l)}}(\boldsymbol{r}) + N_k(r_k)\right]}\right\}^2} - N_{I_k^{(l)}}(\boldsymbol{r}) - N_k(r_k). \tag{94}$$

Claim 3: **If** the SINR falls into the medium-range region between the SINR's high-range and low-range regions specified by Eqs. (91) and (93), respectively, **then** the optimal power allocation policy for the medium-range SINR region, denoted by $\mathcal{P}_k^{\text{OPT,M}}$, at nano transmitter k is given as follows:

$$\mathcal{P}_k^{\text{OPT,M}} = \frac{n}{2}\left\{Q^{-1}(\epsilon_k) + \left\{\left[Q^{-1}(\epsilon_k)\right]^2 + (\log 2)(\lambda_1 - \lambda_2) + n\left[\frac{\mathcal{P}_{\text{total}}(r_k)+1}{N_{I_k^{(l)}}(\boldsymbol{r}) + N_k(r_k)}\right]\right\}^{\frac{1}{2}}\right\}^{-2} - \frac{N_{I_k^{(l)}}(\boldsymbol{r}) + N_k(r_k)}{\mathcal{P}_{\text{total}}(r_k)}. \tag{95}$$

Proof: To derive the closed-form solutions to the optimization problem $\mathbf{P_3}$, we can formulate its Lagrange function, denoted by J, as follows:

$$J = n\left[C(r_k,\mathcal{P}_k) - \sqrt{\frac{V(r_k,\mathcal{P}_k)}{n}}Q^{-1}(\epsilon_k)\right] + \lambda_1\left(\mathcal{P}_k^{\max} - \mathcal{P}_k\right) + \lambda_2\left(\mathcal{P}_k - \mathcal{P}_k^{\min}\right) \tag{96}$$

where λ_1 and λ_2 are the Lagrange multipliers associated with the EH constraints **C2** and **C3** which are specified by Eqs. (77) and (78), respectively, in optimization problem

$\mathbf{P_1}$. Then, we can obtain the following Karush-Kuhn-Tucker (KKT) conditions:

$$\begin{cases} \frac{\partial J}{\partial \mathcal{P}_k} = \frac{n\mathcal{P}_{\text{total}}(r_k)}{2(\log 2)\left[\mathcal{P}_k\mathcal{P}_{\text{total}}(r_k)+N_{I_k^{(l)}}(\boldsymbol{r})+N_k(r_k)\right]} - n(\log_2 e) \\ \qquad \times\left[\frac{\mathcal{P}_{\text{total}}(r_k)+1}{N_{I_k^{(l)}}(\boldsymbol{r})+N_k(r_k)}\right] - \frac{\sqrt{2n}(\log_2 e)Q^{-1}(\epsilon_k)}{\sqrt{\mathcal{P}_k+N_{I_k^{(l)}}(\boldsymbol{r})+N_k(r_k)}} - \lambda_1 + \lambda_2 \\ \qquad = 0; \\ \lambda_1, \lambda_2 > 0. \end{cases} \tag{97}$$

Using the first part of Eq. (97), we can obtain the following equation:

$$\begin{aligned} &\frac{n\mathcal{P}_{\text{total}}(r_k)}{2\left[\mathcal{P}_k\mathcal{P}_{\text{total}}(r_k)+N_{I_k^{(l)}}(\boldsymbol{r})+N_k(r_k)\right]} \\ &\quad - \frac{\sqrt{2n}Q^{-1}(\epsilon_k)}{\sqrt{\mathcal{P}_k+N_{I_k^{(l)}}(\boldsymbol{r})+N_k(r_k)}} \\ &\quad = (\log 2)(\lambda_1-\lambda_2) + n\left[\frac{\mathcal{P}_{\text{total}}(r_k)+1}{N_{I_k^{(l)}}(\boldsymbol{r})+N_k(r_k)}\right]. \end{aligned} \tag{98}$$

To derive the optimal power allocation policy for nano transmitter k, we prove **Claim 1**, **Claim 2**, and **Claim 3**, respectively, for this theorem as follows.

Claim 1: Considering the high-range SINR region, we have $\mathcal{P}_k\mathcal{P}_{\text{total}}(r_k) \gg N_{I_k^{(l)}}(\boldsymbol{r}) + N_k(r_k)$. Since $\mathcal{P}_{\text{total}}(r_k) < 1$, we can obtain:

$$\mathcal{P}_k \gg N_{I_k^{(l)}}(\boldsymbol{r}) + N_k(r_k). \tag{99}$$

As a result, we can convert Eq. (98) in the high-range SINR region into the following equation:

$$\begin{aligned} &\frac{n}{2\mathcal{P}_k} - \frac{\sqrt{2n}Q^{-1}(\epsilon_k)}{\sqrt{\mathcal{P}_k}} \\ &\quad = (\log 2)(\lambda_1-\lambda_2) + n\left[\frac{\mathcal{P}_{\text{total}}(r_k)+1}{N_{I_k^{(l)}}(\boldsymbol{r})+N_k(r_k)}\right]. \end{aligned} \tag{100}$$

By solving Eq. (100), we obtain the optimal power allocation policy $\mathcal{P}_k^{\text{OPT,H}}$ for the high-range SINR region as given in Eq. (92).

Claim 2: In the low-range SINR region, we have $\mathcal{P}_k\mathcal{P}_{\text{total}}(r_k) \ll N_{I_k^{(l)}}(\boldsymbol{r})+N_k(r_k)$. As a result, we can convert Eq. (98) in the low-range SINR region into the following equation:

$$\begin{aligned} &\frac{n\mathcal{P}_{\text{total}}(r_k)}{2\left[N_{I_k^{(l)}}(\boldsymbol{r})+N_k(r_k)\right]} - \frac{\sqrt{2n}Q^{-1}(\epsilon_k)}{\sqrt{\mathcal{P}_k+N_{I_k^{(l)}}(\boldsymbol{r})+N_k(r_k)}} \\ &\quad = (\log 2)(\lambda_1-\lambda_2) + n\left[\frac{\mathcal{P}_{\text{total}}(r_k)+1}{N_{I_k^{(l)}}(\boldsymbol{r})+N_k(r_k)}\right]. \end{aligned} \tag{101}$$

By solving Eq. (101), we can obtain the optimal power allocation policy $\mathcal{P}_k^{\text{OPT,L}}$ for the low-range SINR region as given in Eq. (94).

Claim 3: If the SINR falls into the medium-range region between the high-range and low-range regions of SINR, specified by Eqs. (91) and (93), respectively, then using Eq. (98), we can obtain the following equation:

$$\begin{aligned} &\frac{n\mathcal{P}_{\text{total}}(r_k)}{2\left[\mathcal{P}_k\mathcal{P}_{\text{total}}(r_k)+N_{I_k^{(l)}}(\boldsymbol{r})+N_k(r_k)\right]} \\ &\quad - \frac{\sqrt{2n\mathcal{P}_{\text{total}}(r_k)}Q^{-1}(\epsilon_k)}{\sqrt{\mathcal{P}_k\mathcal{P}_{\text{total}}(r_k)+N_{I_k^{(l)}}(\boldsymbol{r})+N_k(r_k)}} \\ &\quad = (\log 2)(\lambda_1-\lambda_2) + n\left[\frac{\mathcal{P}_{\text{total}}(r_k)+1}{N_{I_k^{(l)}}(\boldsymbol{r})+N_k(r_k)}\right]. \end{aligned} \tag{102}$$

By solving the above Eq. (102), we can obtain the optimal power allocation policy for the medium-range SINR region $\mathcal{P}_k^{\text{OPT,M}}$ as given in Eq. (95). Therefore, we complete the proof for Theorem 5. ■

To ensure the optimality of the resource allocation policy for the optimization problem $\mathbf{P_3}$, we also need to update the Lagrange multipliers λ_1 and λ_2 through iteration. In this paper, we employ the gradient projection method [50] to achieve the renewal of shadow prices due to its faster convergence towards a local extremum compared with other nongradient methods.

Algorithm 1: FBC-EH Based Joint Optimal Resource Allocation Policy

Input: $a, b, B, K, t_{\text{cyc}}, \Delta Q, V_g, C_{\text{cap}}, L_{\max}, P_{\text{circuit}}, \lambda$, and γ_{th}
Initialization: $l = 0$ and $\mathcal{P}_k^{(0)} = \overline{\mathcal{P}}$
for $l = 1, l \le L_{\max}$ **do**
  Step 1:
  Calculate the energy consumption rate by using Eq. (73)
  if $n > n_{\min}$ **then**
    if $\mathcal{P}_k\mathcal{P}_{total}(r_k) \gg N_{I_k^{(l)}}(\boldsymbol{r}) + N_k(r_k)$ **then**
      Calculate the transmit power $\mathcal{P}_k^{(l)}$ that maximize the function $F(n, r_k, \mathcal{P}_k)$ in the high-range SINR region by using Eq. (92)
    else if $\mathcal{P}_k\mathcal{P}_{total}(r_k) \ll N_{I_k^{(l)}}(\boldsymbol{r}) + N_k(r_k)$ **then**
      Calculate the transmit power $\mathcal{P}_k^{(l)}$ that maximize the function $F(n, r_k, \mathcal{P}_k)$ in the low-range SINR region by using Eq. (94)
    else
      Calculate the transmit power $\mathcal{P}_k^{(l)}$ that maximize the function $F(n, r_k, \mathcal{P}_k)$ by using Eq. (95)
    end if
  end if
  Step 2:
  Determine $n^{(l)}$ to increase the FBC-based ϵ-effective capacity $EC_\epsilon^{(l)}(\theta_k)$
  if $l = L_{\max}$ **then**
    $\mathcal{P}_k^{\text{OPT}} \leftarrow \mathcal{P}_k^{(l)}$ and $n_k^{\text{OPT}} \leftarrow n_k^{(l)}$, $\forall \mathcal{P}_k^{\text{OPT}} \in \left\{\mathcal{P}_k^{\text{OPT,H}}, \mathcal{P}_k^{\text{OPT,M}}, \mathcal{P}_k^{\text{OPT,L}}\right\}$
  end if
  Update the Lagrange multipliers $\lambda_1^{(l)}$ and $\lambda_2^{(l)}$ as specified by Eq. (104)
  $l \leftarrow (l+1)$
end for

We define

$$\begin{cases} \mathcal{P}_k^{\max} \triangleq \min\left\{ \frac{C_{\text{cap}} V_g}{2n\zeta_k} - \frac{P_{\text{circuit}}}{\zeta_k}, \frac{V_g \Delta Q}{nC(r_k,\mathcal{P}_k)t_{\text{cyc}}} \left[\exp\left(-\frac{\Delta Q n_{\text{cyc}}}{V_g C_{\text{cap}}}\right) \right.\right. \\ \qquad \left.\left. - \exp\left(-\frac{2\Delta Q n_{\text{cyc}}}{V_g C_{\text{cap}}}\right) \right] \right\}; \\ \mathcal{P}_k^{\min} \triangleq \frac{1}{(r_k)^{-\eta} G 10^{\frac{\xi_k}{10}} S(f)} \left[\frac{\gamma_{\text{th}}\left(N_k(r_k) + N_{I_k^{(l)}}(\boldsymbol{r})\right)}{\left(\frac{c}{4\pi f r_k}\right) e^{-\frac{\alpha_{\text{abs}} r_k}{2}}} \right]^2. \end{cases} \tag{103}$$

Denote by l the number of current iteration and consider $\lambda_1^{(l)}$ and $\lambda_2^{(l)}$ the Lagrange multipliers at the lth iteration, respectively. To be specific, the Lagrange multipliers $\lambda_1^{(l)}$ and $\lambda_2^{(l)}$ can be updated as follows:

$$\begin{cases} \lambda_1^{(l+1)} = \left[\lambda_1^{(l)} + \tau_1 \left(\mathcal{P}_k^{\max} - \mathcal{P}_k\right)\right]^+; \\ \lambda_2^{(l+1)} = \left[\lambda_2^{(l)} + \tau_2 \left(\mathcal{P}_k - \mathcal{P}_k^{\min}\right)\right]^+, \end{cases} \tag{104}$$

where $[a]^+ = \max\{a, 0\}$ and τ_1 and τ_2 are the positive step sizes. Define $L_{\max}$ as the maximum iteration number. Denote by $n^{(l)}$, $\mathcal{P}_k^{(l)}$, and $EC_\epsilon^{(l)}(\theta_k)$ the blocklength, transmit power, and ϵ-effective capacity at the lth iteration, respectively. Define n_k^{OPT} as the optimal blocklength and also we define $\mathcal{P}_k^{\text{OPT}} \in \left\{\mathcal{P}_k^{\text{OPT,H}}, \mathcal{P}_k^{\text{OPT,M}}, \mathcal{P}_k^{\text{OPT,L}}\right\}$ as the general notation of the optimal power allocation policy for nano transmitter k in the THz band. To solve the optimization problem $\mathbf{P_1}$, we develop the FBC-EH based optimal resource allocation policy as shown in **Algorithm 1** for our proposed statistical delay and error-rate bounded QoS provisioning in supporting mURLLC over FBC-EH based 6G THz wireless nano-networks.

V. Performance Evaluations

We use MATLAB-based simulations to validate and evaluate our proposed FBC-EH based 6G THz wireless nano-networks under statistical delay and error-rate bounded QoS provisioning. Throughout our simulations, we set the bandwidth $B = 1$ THz, the radius of the THz-band covered region $a = 5$ m, the radius of the blind area $b = 5$ mm, the reference temperature $T_0 = 310K$, and the SINR threshold $\gamma_{\text{th}} = 10$ dB. In light of the state-of-the-art in molecular-electronics, we set the total signal energy to be 500 pJ, which is independent of the power spectral distribution. For our proposed THz-band FBC-EH-based nano-communication schemes, we set the generator voltage $V_g = 0.42$ V, total capacitance $C_{\text{cap}} = 176$ μF, the amount of electric charge per cycle $\Delta Q = 3.63$ nC, and the average time between vibrations $t_{\text{cyc}} = 0.02$ sec [44] [45].

Figure 3 plots the aggregate interference power as a function of the nano node density λ for our proposed schemes. We can observe from Fig. 3 that the aggregate interference first increases and finally converges to a certain value as the node density λ increases. This implies that compared to the interference, the effect of molecular absorption noise is of the secondary importance for our proposed THz-band wireless nano-networks as $K \to \infty$. Fig. 3 also shows that given the same node density λ, the aggregate interference decreases at higher frequency f. This implies that the path loss is proportional to the square of frequency f and the absorption coefficients are usually larger at higher frequency in the THz band.

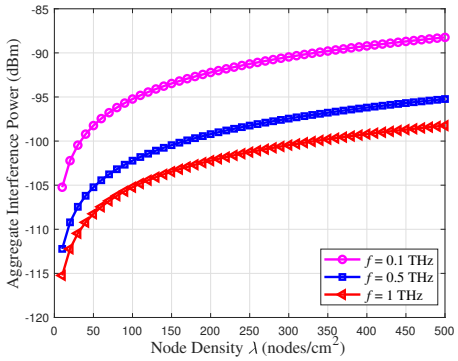

Fig. 3. The aggregate interference power (dBm) vs. node density λ in the THz band.

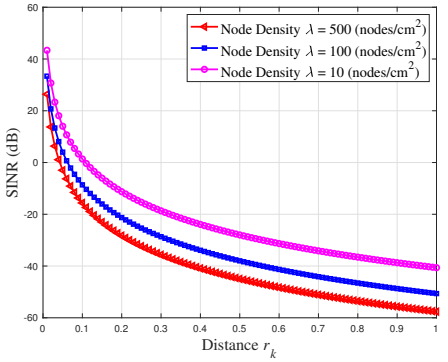

Fig. 4. The SINR (dB) vs. transmission distance r_k in the THz band in the finite blocklength regime.

Setting the frequency $f = 1$ THz, using Eq. (20), Fig. 4 plots the SINR $\gamma_k^{(l)}(\boldsymbol{r})$ as a function of the transmission distance r_k for our proposed schemes. We can observe from Fig. 4 that the SINR $\gamma_k^{(l)}(\boldsymbol{r})$ first decreases and then converges to a certain value as the transmission distance r_k increases. This implies that with a shorter transmission distance, we have a lower path loss, which leads to a larger value of the SINR. Fig. 4 shows that the SINR $\gamma_k^{(l)}(\boldsymbol{r})$ decreases as the node density λ increases, indicating that the node density is limited for the practical applications of wireless nano-networks.

Using Eqs. (52) and (54), Fig. 5 depicts the channel capacity $C(r_k, \mathcal{P}_k)$ with different blocklengths n in the THz band for our proposed schemes. As shown in Fig. 5, the channel capacity $C(r_k, \mathcal{P}_k)$ increases as the blocklength n increases. Fig. 5 also shows that the channel capacity $C(r_k, \mathcal{P}_k)$ decreases as the transmission distance r_k increases.

Given different blocklengths n, Fig. 6 depicts the ϵ-effective capacity $EC_\epsilon(\theta_k)$ as a function of QoS exponent θ_k in the THz band for our proposed schemes. We can observe from Fig. 6 that the ϵ-effective capacity $EC_\epsilon(\theta_k)$ decreases as

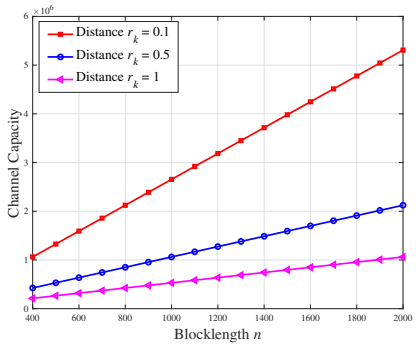

Fig. 5. The channel capacity $C(r_k, \mathcal{P}_k)$ vs. blocklength n in the THz band in the finite blocklength regime.

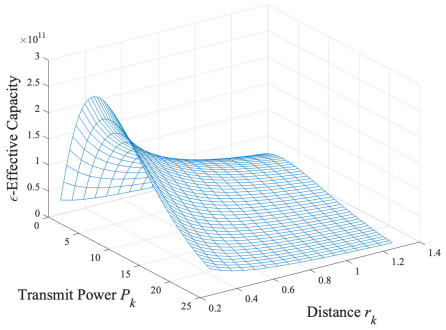

Fig. 8. The ϵ-effective capacity $EC_\epsilon(\theta_k)$ vs. transmit power $\mathcal{P}_k$ and transmission distance r_k in the THz band in the finite blocklength regime.

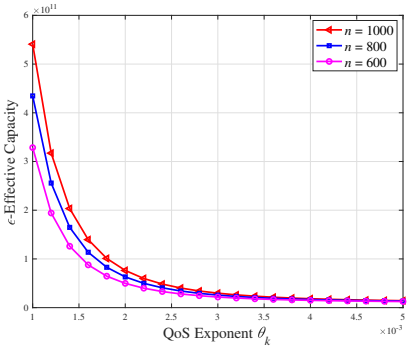

Fig. 6. The ϵ-effective capacity $EC_\epsilon(\theta_k)$ vs. QoS exponent θ_k in the THz band in the finite blocklength regime.

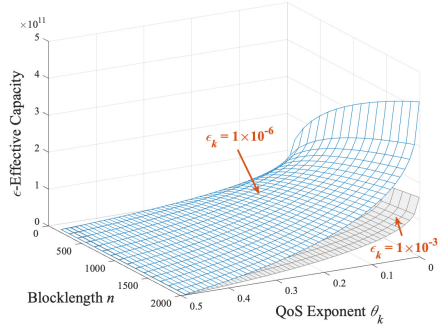

Fig. 9. The ϵ-effective capacity $EC_\epsilon(\theta_k)$ vs. blocklength n and QoS exponent θ_k in the THz band in the finite blocklength regime.

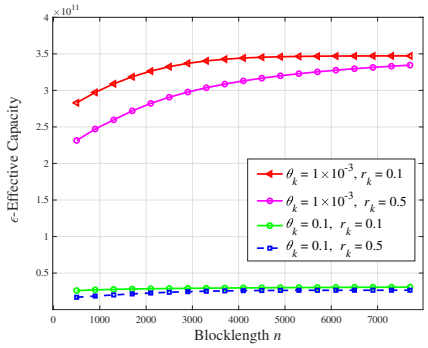

Fig. 7. The ϵ-effective capacity $EC_\epsilon(\theta_k)$ vs. blocklength n in the THz band in the finite blocklength regime.

the QoS exponent θ_k increases. We can also observe that the gaps among each curve decrease as the QoS exponent θ_k increases. Fig. 6 also shows that the ϵ-effective capacity $EC_\epsilon(\theta_k)$ increases as the blocklength n increases.

Setting the frequency $f = 1$ THz and node density $\lambda = 100$ nodes/cm^2, Fig. 7 plots the ϵ-effective capacity $EC_\epsilon(\theta_k)$ as a function of the blocklength n in the THz band using FBC. We can observe from Fig. 7 that the ϵ-effective capacity $EC_\epsilon(\theta_k)$ increases as the blocklength n increases and will converge to a certain value as $n \to \infty$. Fig. 7 also shows that the value of the ϵ-effective capacity $EC_\epsilon(\theta_k)$ depends on the transmission distance r_k.

Figure 8 depicts the ϵ-effective capacity $EC_\epsilon(\theta_k)$ as a function of both transmit power $\mathcal{P}_k$ (pJ) and transmission distance r_k in the THz band. We can observe from Fig. 8 that there exists an optimal transmit power $\mathcal{P}_k^{\text{OPT}}$ that maximizes the ϵ-effective capacity $EC_\epsilon(\theta_k)$. Fig. 8 also shows that the optimal transmit power $\mathcal{P}_k^{\text{OPT}}$ depends on the transmission distance r_k. With the increase of the transmission distance, the value of the optimal transmit power $\mathcal{P}_k^{\text{OPT}}$ decreases in order to achieve the maximum ϵ-effective capacity $EC_\epsilon(\theta_k)$. In addition, setting the frequency $f = 0.1$ THz and the transmission distance $r_k = 0.5$, Fig. 9 plots the ϵ-effective capacity $EC_\epsilon(\theta_k)$ as a function of both blocklength n and QoS exponent θ_k for our proposed schemes. We can observe from Fig. 9 that a smaller QoS exponent θ_k achieves a larger value of ϵ-effective capacity $EC_\epsilon(\theta_k)$ in the THz band. This implies that a smaller QoS exponent $\theta_k \to 0$ and a larger QoS exponent $\theta_k \to \infty$ set an upper bound and lower bound on the ϵ-effective capacity, respectively.

VI. Conclusions

We have developed the optimal resource allocation policies to maximize the ϵ-effective capacity in the THz band over EH-based wireless nano-networks in the finite blocklength regime for statistical delay and error-rate bounded QoS provisioning. In particular, we have established EH-based THz-band nano-communication system models in the finite blocklength regime. Then, we have analyzed the THz-band aggregate interference, channel capacity, and channel dispersion func-

tions using FBC. Considering statistical delay and error-rate bounded QoS provisioning, we have formulated and solved the ϵ-effective capacity maximization problem for our proposed statistical delay and error-rate bounded QoS provisioning in supporting mURLLC over FBC-EH based 6G THz wireless nano-networks. Simulation results are included, which validate and evaluate our proposed schemes in the THz band over wireless nano-networks.

REFERENCES

[1] Xi Zhang, Jia Tang, Hsiao-Hwa Chen, Song Ci, and M. Guizani, "Cross-layer-based modeling for quality of service guarantees in mobile wireless networks," *IEEE Communications Magazine*, vol. 44, no. 1, pp. 100–106, 2006.

[2] J. Tang and X. Zhang, "Quality-of-service driven power and rate adaptation over wireless links," *IEEE Transactions on Wireless Communications*, vol. 6, no. 8, pp. 3058–3068, 2007.

[3] ——, "Cross-layer resource allocation over wireless relay networks for quality of service provisioning," *IEEE Journal on Selected Areas in Communications*, vol. 25, no. 4, pp. 645–656, May 2007.

[4] ——, "Cross-layer modeling for quality of service guarantees over wireless links," *IEEE Transactions on Wireless Communications*, vol. 6, no. 12, pp. 4504–4512, 2007.

[5] ——, "Quality-of-service driven power and rate adaptation for multichannel communications over wireless links," *IEEE Transactions on Wireless Communications*, vol. 6, no. 12, pp. 4349–4360, 2007.

[6] X. Zhang and Q. Du, "Cross-layer modeling for QoS-driven multimedia multicast/broadcast over fading channels in [advances in mobile multimedia]," *IEEE Communications Magazine*, vol. 45, no. 8, pp. 62–70, 2007.

[7] H. Su and X. Zhang, "Cross-layer based opportunistic MAC protocols for QoS provisionings over cognitive radio wireless networks," *IEEE Journal on Selected Areas in Communications*, vol. 26, no. 1, pp. 118–129, Jan. 2008.

[8] W. Cheng, X. Zhang, and H. Zhang, "Heterogeneous statistical QoS provisioning for downlink transmissions over mobile wireless cellular networks," in *Proc. IEEE GLOBECOM 2014*, 2014, pp. 4757–4763.

[9] W. Saad, M. Bennis, and M. Chen, "A vision of 6G wireless systems: applications, trends, technologies, and open research problems," *IEEE Network*, vol. 34, no. 3, pp. 134–142, 2020.

[10] K. B. Letaief, W. Chen, Y. Shi, J. Zhang, and Y. A. Zhang, "The roadmap to 6G: AI empowered wireless networks," *IEEE Communications Magazine*, vol. 57, no. 8, pp. 84–90, August 2019.

[11] Z. Zhang, Y. Xiao, Z. Ma, M. Xiao, Z. Ding, X. Lei, G. K. Karagiannidis, and P. Fan, "6G wireless networks: vision, requirements, architecture, and key technologies," *IEEE Vehicular Technology Magazine*, vol. 14, no. 3, pp. 28–41, September 2019.

[12] Y. Polyanskiy, H. V. Poor, and S. Verdú, "Channel coding rate in the finite blocklength regime," *IEEE Transactions on Information Theory*, vol. 56, no. 5, pp. 2307–2359, May 2010.

[13] G. Ozcan and M. C. Gursoy, "Throughput of cognitive radio systems with finite blocklength codes," *IEEE Journal on Selected Areas in Communications*, vol. 31, no. 11, pp. 2541–2554, 2013.

[14] S. Xu, T. Chang, S. Lin, C. Shen, and G. Zhu, "Energy-efficient packet scheduling with finite blocklength codes: convexity analysis and efficient algorithms," *IEEE Transactions on Wireless Communications*, vol. 15, no. 8, pp. 5527–5540, Aug. 2016.

[15] P. Mary, J. Gorce, A. Unsal, and H. V. Poor, "Finite blocklength information theory: What is the practical impact on wireless communications?" in *Proc. IEEE Globecom Workshops*, 2016, pp. 1–6.

[16] Y. Polyanskiy and S. Verdú, "Empirical distribution of good channel codes with non-vanishing error probability," *IEEE transactions on information theory*, vol. 60, no. 1, pp. 5–21, 2013.

[17] Y. Polyanskiy, H. V. Poor, and S. Verdú, "Feedback in the non-asymptotic regime," *IEEE Transactions on Information Theory*, vol. 57, no. 8, pp. 4903–4925, Aug. 2011.

[18] T. Kürner and S. Priebe, "Towards THz communications-status in research, standardization and regulation," *Journal of Infrared, Millimeter, and Terahertz Waves*, vol. 35, no. 1, pp. 53–62, 2014.

[19] M. Božanić and S. Sinha, *Millimeter-Wave Integrated Circuits: methodologies for Research, Design and Innovation*. Springer Nature, 2020, vol. 658.

[20] I. Akyildiz, J. Jornet, and C. Han, "Terahertz band: next frontier for wireless communications," *Physical Communication*, vol. 12, pp. 16–32, 2014.

[21] J. M. Jornet and I. F. Akyildiz, "Low-weight channel coding for interference mitigation in electromagnetic nanonetworks in the Terahertz band," in *Proc. 2011 IEEE International Conference on Communications (ICC)*, 2011, pp. 1–6.

[22] H. Song and T. Nagatsuma, "Present and future of Terahertz communications," *IEEE Transactions on Terahertz Science and Technology*, vol. 1, no. 1, pp. 256–263, Sep. 2011.

[23] K. S. Novoselov, L. C. V. Fal, P. Gellert, M. Schwab, and K. Kim, "A roadmap for graphene," *Nature*, vol. 490, no. 7419, pp. 192–200, 2012.

[24] H. A. Hafez, S. Kovalev, J.-C. Deinert, Z. Mics, B. Green, N. Awari, M. Chen, S. Germanskiy, U. Lehnert, J. Teichert, Z. Wang, K.-J. Tielrooij, Z. Liu, Z. Chen, A. Narita, K. Mllen, M. Bonn, M. Gensch, and D. Turchinovich, "Extremely efficient Terahertz high-harmonic generation in graphene by hot dirac fermions," *Nature*, vol. 561, no. 7724, pp. 507–511, 2018.

[25] I. F. Akyildiz and J. M. Jornet, "The Internet of nano-things," *IEEE Wireless Communications*, vol. 17, no. 6, pp. 58–63, 2010.

[26] Q. H. Abbasi, H. El Sallabi, N. Chopra, K. Yang, K. A. Qaraqe, and A. Alomainy, "Terahertz channel characterization inside the human skin for nano-scale body-centric networks," *IEEE Transactions on Terahertz Science and Technology*, vol. 6, no. 3, pp. 427–434, 2016.

[27] Z. Xu, X. Dong, and J. Bornemann, "Design of a reconfigurable MIMO system for THz communications based on graphene antennas," *IEEE Transactions on Terahertz Science and Technology*, vol. 4, no. 5, pp. 609–617, 2014.

[28] ——, "Spectral efficiency of carbon nanotube antenna based MIMO systems in the Terahertz band," *IEEE Wireless Communications Letters*, vol. 2, no. 6, pp. 631–634, 2013.

[29] Q. H. Abbasi, K. Yang, N. Chopra, J. M. Jornet, N. A. Abuali, K. A. Qaraqe, and A. Alomainy, "Nano-communication for biomedical applications: A review on the state-of-the-art from physical layers to novel networking concepts," *IEEE Access*, vol. 4, pp. 3920–3935, 2016.

[30] F. Dressler and S. Fischer, "Connecting in-body nano communication with body area networks: challenges and opportunities of the internet of nano things," *Nano Communication Networks*, vol. 6, no. 2, pp. 29–38, 2015.

[31] F. Afsana, M. Asif-Ur-Rahman, M. R. Ahmed, M. Mahmud, and M. S. Kaiser, "An energy conserving routing scheme for wireless body sensor nanonetwork communication," *IEEE Access*, vol. 6, pp. 9186–9200, 2018.

[32] J. M. Jornet and I. F. Akyildiz, "Channel modeling and capacity analysis for electromagnetic wireless nanonetworks in the Terahertz band," *IEEE Transactions on Wireless Communications*, vol. 10, no. 10, pp. 3211–3221, Oct. 2011.

[33] J. M. Jornet and I. F. Akyildiz, "Channel capacity of electromagnetic nanonetworks in the Terahertz band," in *Proc. 2010 IEEE International Conference on Communications*, 2010, pp. 1–6.

[34] S. Sudevalayam and P. Kulkarni, "Energy harvesting sensor nodes: survey and implications," *IEEE Communications Surveys Tutorials*, vol. 13, no. 3, pp. 443–461, 2011.

[35] V. Sharma, U. Mukherji, V. Joseph, and S. Gupta, "Optimal energy management policies for energy harvesting sensor nodes," *IEEE Transactions on Wireless Communications*, vol. 9, no. 4, pp. 1326–1336, 2010.

[36] A. Baddeley, I. Bárány, and R. Schneider, *Stochastic Geometry: lectures Given at the CIME Summer School Held in Martina Franca, Italy, September 13-18, 2004*. Springer, 2006.

[37] V. Petrov, D. Moltchanov, and Y. Koucheryavy, "Interference and SINR in dense terahertz networks," in *2015 IEEE 82nd Vehicular Technology Conference (VTC2015-Fall)*, 2015, pp. 1–5.

[38] F. Afsana, S. A. Mamun, M. S. Kaiser, and M. R. Ahmed, "Outage capacity analysis of cluster-based forwarding scheme for body area network using nano-electromagnetic communication," in *Proc. 2015 2nd International Conference on Electrical Information and Communication Technologies (EICT)*, 2015, pp. 383–388.

[39] I. Llatser, A. Cabellos-Aparicio, E. Alarcn, J. M. Jornet, A. Mestres, H. Lee, and J. Solé-Pareta, "Scalability of the channel capacity in graphene-enabled wireless communications to the nanoscale," *IEEE Transactions on Communications*, vol. 63, no. 1, pp. 324–333, Jan. 2015.

[40] R. Zhang, K. Yang, Q. Abbasi, K. Qaraqe, and A. Alomainy, "Analytical modelling of the effect of noise on the Terahertz in-vivo communication channel for body-centric nano-networks," *Nano Communication Networks*, vol. 15, pp. 59–68, May 2017.

[41] S. Chandrasekhar, *Radiative Transfer*. Courier Corporation, 2013.

[42] S. Xu, B. J. Hansen, and Z. L. Wang, "Piezoelectric-nanowire-enabled

power source for driving wireless microelectronics," *Nature Communications*, vol. 1, no. 7, pp. 1–5, Oct. 2010.
[43] S. Xu, Y. Qin, C. Xu, Y. Wei, R. Yang, and Z. L. Wang, "Self-powered nanowire devices," *Nature Nanotechnology*, vol. 5, pp. 366–373, 2010.
[44] J. M. Jornet and I. F. Akyildiz, "Joint energy harvesting and communication analysis for perpetual wireless nanosensor networks in the Terahertz band," *IEEE Transactions on Nanotechnology*, vol. 11, no. 3, pp. 570–580, 2012.
[45] J. M. Jornet, "A joint energy harvesting and consumption model for self-powered nano-devices in nanonetworks," in *Proc. 2012 IEEE International Conference on Communications (ICC)*, 2012, pp. 6151–6156.
[46] E. MolavianJazi and J. N. Laneman, "A random coding approach to Gaussian multiple access channels with finite blocklength," in *Proc. 2012 50th Annual Allerton Conference on Communication, Control, and Computing (Allerton)*, 2012, pp. 286–293.
[47] V. Petrov, D. Moltchanov, and Y. Koucheryavy, "Interference and SINR in dense Terahertz networks," in *Proc. 2015 IEEE 82nd Vehicular Technology Conference (VTC2015-Fall)*, 2015, pp. 1–5.
[48] R. S. Ellis, *Entropy, Large Deviations, and Statistical Mechanics*. Springer-Verlag, Berlin, Heidelberg, New York, Tokyo, 2007.
[49] J. Tang and X. Zhang, "Cross-layer-model based adaptive resource allocation for statistical QoS guarantees in mobile wireless networks," *IEEE Transactions on Wireless Communications*, vol. 7, no. 6, pp. 2318–2328, 2008.
[50] S. Boyd, L. Xiao, and A. Mutapcic, "Subgradient methods," *lecture notes of EE392o, Stanford University, Autumn Quarter*, pp. 2004–2005, 2003.

Xi Zhang (Fellow, IEEE) received the B.S. and M.S. degrees from Xidian University, Xi'an, China, the M.S. degree from Lehigh University, Bethlehem, PA, all in electrical engineering and computer science, and the Ph.D. degree in electrical engineering and computer science (Electrical Engineering-Systems) from The University of Michigan, Ann Arbor, MI, USA.

He is currently a Full Professor and the Founding Director of the Networking and Information Systems Laboratory, Department of Electrical and Computer Engineering, Texas A&M University, College Station. He is a Fellow of the IEEE for contributions to quality of service (QoS) theory in mobile wireless networks. He was with the Networks and Distributed Systems Research Department, AT&T Bell Laboratories, Murray Hill, New Jersey, and AT&T Laboratories Research, Florham Park, New Jersey, in 1997. He was a research fellow with the School of Electrical Engineering, University of Technology, Sydney, Australia, and the Department of Electrical and Computer Engineering, James Cook University, Australia. He has published more than 400 research papers on wireless networks and communications systems, network protocol design and modeling, statistical communications, random signal processing, information theory, and control theory and systems. He is an IEEE Distinguished Lecturer of both IEEE Communications Society and IEEE Vehicular Technology Society. He also received the TEES Select Young Faculty Award for Excellence in Research Performance from the Dwight Look College of Engineering at Texas A&M University, College Station, in 2006 and the Outstanding Faculty Award from Department of Electrical and Computer Engineering, Texas A&M University, in 2020. He received the U.S. National Science Foundation CAREER Award in 2004 for his research in the areas of mobile wireless and multicast networking and systems. He received six Best Paper Awards at IEEE GLOBECOME 2020, IEEE ICC 2018, IEEE GLOBECOM 2014, IEEE GLOBECOM 2009, IEEE GLOBECOM 2007, and IEEE WCNC 2010, respectively. One of his IEEE Journal on Selected Areas in Communications papers has been listed as the IEEE Best Readings Paper (receiving the highest citation rate among all IEEE Transactions/Journal papers in the area) on Wireless Cognitive Radio Networks and Statistical QoS Provisioning over Mobile Wireless Networking.

Professor Zhang is serving or has served as an Editor for IEEE TRANSACTIONS ON COMMUNICATIONS, IEEE TRANSACTIONS ON WIRELESS COMMUNICATIONS, IEEE TRANSACTIONS ON VEHICULAR TECHNOLOGY, IEEE TRANSACTIONS ON GREEN COMMUNICATIONS AND NETWORKING, and IEEE TRANSACTIONS ON NETWORK SCIENCE AND ENGINEERING, twice as a Guest Editor for IEEE JOURNAL ON SELECTED AREAS IN COMMUNICATIONS for two special issues on "Broadband Wireless Communications for High Speed Vehicles" and "Wireless Video Transmissions," an Associate Editor for IEEE COMMUNICATIONS LETTERS, twice as the Lead Guest Editor for *IEEE Communications Magazine* for two special issues on "Advances in Cooperative Wireless Networking" and "Underwater Wireless Communications and Networks: Theory and Applications," a Guest Editor for *IEEE Wireless Communications Magazine* for special issue on "Next Generation CDMA vs. OFDMA for 4G Wireless Applications," an Editor for Wiley's JOURNAL ON WIRELESS COMMUNICATIONS AND MOBILE COMPUTING, JOURNAL OF COMPUTER SYSTEMS, NETWORKING, AND COMMUNICATIONS, and Wiley's JOURNAL ON SECURITY AND COMMUNICATIONS NETWORKS, and an Area Editor for Elsevier's JOURNAL ON COMPUTER COMMUNICATIONS, among many others. He is serving or has served as the TPC Chair for IEEE GLOBECOM 2011, TPC Vice-Chair for IEEE INFOCOM 2010, TPC Area Chair for IEEE INFOCOM 2012, Panel/Demo/Poster Chair for ACM MobiCom 2011, General Chair for IEEE WCNC 2013, and TPC Chair for IEEE INFOCOM 2017-2019 Workshops on "Integrating Edge Computing, Caching, and Offloading in Next Generation Networks," etc.

Jingqing Wang received the B.S. degree from Northwestern Polytechnical University, Xi'an, China, in Electronics and Information Engineering. She is currently pursuing her Ph.D. degree under the supervision of Professor Xi Zhang in Networking and Information Systems Laboratory, Department of Electrical and Computer Engineering, Texas A&M University, College Station, TX, USA. She won the Best Paper Award from the IEEE GLOBECOM in 2020 and 2014, respectively, the Hagler Institute for Advanced Study Heep Graduate Fellowship Award from Texas A&M University in 2018, and Dr. R.K. Pandey and Christa U. Pandey'84 Fellowship, Texas A&M University, USA, 2020-2021. Her research interests focus on big data based 5G and beyond mobile wireless networks technologies, statistical delay and error-rate bounded QoS provisioning, 6G mURLLC, information-theoretic analyses of FBC, emerging machine learning techniques over 5G and beyond mobile wireless networks.

H. Vincent Poor (Life Fellow, IEEE) received the Ph.D. degree in EECS from Princeton University in 1977. From 1977 until 1990, he was on the faculty of the University of Illinois at Urbana-Champaign. Since 1990 he has been on the faculty at Princeton, where he is currently the Michael Henry Strater University Professor. During 2006 to 2016, he served as the dean of Princeton's School of Engineering and Applied Science. He has also held visiting appointments at several other universities, including most recently at Berkeley and Cambridge. His research interests are in the areas of information theory, machine learning and network science, and their applications in wireless networks, energy systems and related fields. Among his publications in these areas is the forthcoming book *Machine Learning and Wireless Communications*. (Cambridge University Press, 2021).

Dr. Poor is a member of the National Academy of Engineering and the National Academy of Sciences and is a foreign member of the Chinese Academy of Sciences, the Royal Society, and other national and international academies. Recent recognition of his work includes the 2017 IEEE Alexander Graham Bell Medal and a D.Eng. *honoris causa* from the University of Waterloo awarded in 2019.